U S ARMY NATICK LABORATORIES

TECHNICAL REPORT

C&OM-I

A PHOTO-OPTICAL SYSTEM FOR THE MEASUREMENT OF PROJECTILE VELOCITY

CLOTHING & ORGANIC MATERIALS DIVISION

OCTOBER 1963

NATICK, MASSACHUSETTS

AD-	Div. 24	Accession No.	UNCLASSIFIED

U.S. Army Natick Laboratories, Natick, Mass. A PHOTO-OPTICAL SYSTEM FOR THE MEASUREMENT OF PROJECTILE VELOCITY by Stanley D. Tanenholtz. Oct 1963, 57 pp illus (Technical Report C&OM 1)

A photo-optical system has been developed for determining the velocity of a projectile after target penetration. This system provides a wide field of view and overcomes the difficulties introduced by light from the projectile-target impact and by the pretriggering of velocity-measuring transducers by particles broken from the target.

The system employs a parallel-light shadowgraphic method that consists of a double-spark source at the focal point of a converging Fresnel lens, and a similar lens to focus the light into a camera. The system is activated by the projectile which, after penetrating the target, triggers a transducer whose pulse is fed to a delay unit. The delay unit in turn triggers the spark unit when the projectile is within the parallel-light field. The result is a shadowgraph of the projectile and the accompanying punch-out material in two positions. The distance between the two images on the photograph (corrected by a suitable magnification factor) divided by the spark time interval gives the average velocity of the projectile.

This [illegible] enables the measurement of residual velocity with an err r of [illegible] 1 to 2 percent and, at the same time, permits the observation of size, shape, distribution of other particles, and distortion of the projectile.

1. High-speed photography
2. Ballistics
3. Photographic analysis
4. Impact shock
5. Velocity
6. Terminal ballistics
7. Projectile trajectories
8. Ballistic cameras
9. Shock waves

I. Title
II. Tanenholtz, Stanley D.
III. Series

AD-	Div. 24	Accession No.	UNCLASSIFIED

U.S. Army Natick Laboratories, Natick, Mass. A PHOTO-OPTICAL SYSTEM FOR THE MEASUREMENT OF PROJECTILE VELOCITY by Stanley D. Tanenholtz. Oct 1963, 57 pp illus (Technical Report C&OM 1)

A photo-optical system has been developed for determining the velocity of a projectile after target penetration. This system provides a wide field of view and overcomes the difficulties introduced by light from the projectile-target impact and by the pretriggering of velocity-measuring transducers by particles broken from the target.

The system employs a parallel-light shadowgraphic method that consists of a double-spark source at the focal point of a converging Fresnel lens, and a similar lens to focus the light into a camera. The system is activated by the projectile which, after penetrating the target, triggers a transducer whose pulse is fed to a delay unit. The delay unit in turn triggers the spark unit when the projectile is within the parallel-light field. The result is a shadowgraph of the projectile and the accompanying punch-out material in two positions. The distance between the two images on the photograph (corrected by a suitable magnification factor) divided by the spark time interval gives the average velocity of the projectile.

This system enables the measurement of residual velocity with an error of only 1 to 2 percent and, at the same time, permits the observation of size, shape, distribution of other particles, and distortion of the projectile.

1. High-speed photography
2. Ballistics
3. Photographic analysis
4. Impact shock
5. Velocity
6. Terminal ballistics
7. Projectile trajectories
8. Ballistic cameras
9. Shock waves

I. Title
II. Tanenholtz, Stanley D.
III. Series

AD-	Div. 24	Accession No.	UNCLASSIFIED

U.S. Army Natick Laboratories, Natick, Mass. A PHOTO-OPTICAL SYSTEM FOR THE MEASUREMENT OF PROJECTILE VELOCITY by Stanley D. Tanenholtz. Oct 1963, 57 pp illus (Technical Report C&OM 1)

A photo-optical system has been developed for determining the velocity of a projectile after target penetration. This system provides a wide field of view and overcomes the difficulties introduced by light from the projectile-target impact and by the pretriggering of velocity-measuring transducers by particles broken from the target.

The system employs a parallel-light shadowgraphic method that consists of a double-spark source at the focal point of a converging Fresnel lens, and a similar lens to focus the light into a camera. The system is activated by the projectile which, after penetrating the target, triggers a transducer whose pulse is fed to a delay unit. The delay unit in turn triggers the spark unit when the projectile is within the parallel-light field. The result is a shadowgraph of the projectile and the accompanying punch-out material in two positions. The distance between the two images on the photograph (corrected by a suitable magnification factor) divided by the spark time interval gives the average velocity of the projectile.

This system enables the measurement of residual velocity with an error of only 1 to 2 percent and, at the same time, permits the observation of size, shape, distribution of other particles, and distortion of the projectile.

1. High-speed photography
2. Ballistics
3. Photographic analysis
4. Impact shock
5. Velocity
6. Terminal ballistics
7. Projectile trajectories
8. Ballistic cameras
9. Shock waves

I. Title
II. Tanenholtz, Stanley D.
III. Series

AD-	Div. 24	Accession No.	UNCLASSIFIED

U.S. Army Natick Laboratories, Natick, Mass. A PHOTO-OPTICAL SYSTEM FOR THE MEASUREMENT OF PROJECTILE VELOCITY by Stanley D. Tanenholtz. Oct 1963, 57 pp illus (Technical Report C&OM 1)

A photo-optical system has been developed for determining the velocity of a projectile after target penetration. This system provides a wide field of view and overcomes the difficulties introduced by light from the projectile-target impact and by the pretriggering of velocity-measuring transducers by particles broken from the target.

The system employs a parallel-light shadowgraphic method that consists of a double-spark source at the focal point of a converging Fresnel lens, and a similar lens to focus the light into a camera. The system is activated by the projectile which, after penetrating the target, triggers a transducer whose pulse is fed to a delay unit. The delay unit in turn triggers the spark unit when the projectile is within the parallel-light field. The result is a shadowgraph of the projectile and the accompanying punch-out material in two positions. The distance between the two images on the photograph (corrected by a suitable magnification factor) divided by the spark time interval gives the average velocity of the projectile.

This system enables the measurement of residual velocity with an error of only 1 to 2 percent and, at the same time, permits the observation of size, shape, distribution of other particles, and distortion of the projectile.

1. High-speed photography
2. Ballistics
3. Photographic analysis
4. Impact shock
5. Velocity
6. Terminal ballistics
7. Projectile trajectories
8. Ballistic cameras
9. Shock waves

I. Title
II. Tanenholtz, Stanley D.
III. Series

AD- Div. 24 Accession No. UNCLASSIFIED

U.S. Army Natick Laboratories, Natick, Mass. A PHOTO-OPTICAL SYSTEM FOR THE MEASUREMENT OF PROJECTILE VELOCITY by Stanley D. Tanenholtz. Oct 1963, 57 pp illus (Technical Report C&OM 1)

A photo-optical system has been developed for determining the velocity of a projectile after target penetration. This system provides a wide field of view and overcomes the difficulties introduced by light from the projectile-target impact and by the pretriggering of velocity-measuring transducers by particles broken from the target.

The system employs a parallel-light shadowgraphic method that consists of a double-spark source at the focal point of a converging Fresnel lens, and a similar lens to focus the light into a camera. The system is activated by the projectile which, after penetrating the target, triggers a transducer whose pulse is fed to a delay unit. The delay unit in turn triggers the spark unit when the projectile is within the parallel-light field. The result is a shadowgraph of the projectile and the accompanying punch-out material in two positions. The distance between the two images on the photograph (corrected by a suitable magnification factor) divided by the spark interval gives the average velocity of the projectile.

This system enables the measurement of residual velocity with an error of only 1 to 2 percent and, at the same time, permits the observation of size, shape, distribution of other particles, and distortion of the projectile.

1. High-speed photography
2. Ballistics
3. Photographic analysis
4. Impact shock
5. Velocity
6. Terminal ballistics
7. Projectile trajectories
8. Ballistic cameras
9. Shock waves

I. Title
II. Taneholtz, Stanley D.
III. Series

AD- Div. 24 Accession No. UNCLASSIFIED

U.S. Army Natick Laboratories, Natick, Mass. A PHOTO-OPTICAL SYSTEM FOR THE MEASUREMENT OF PROJECTILE VELOCITY by Stanley D. Tanenholtz. Oct 1963, 57 pp illus (Technical Report C&OM 1)

A photo-optical system has been developed for determining the velocity of a projectile after target penetration. This system provides a wide field of view and overcomes the difficulties introduced by light from the projectile-target impact and by the pretriggering of velocity-measuring transducers by particles broken from the target.

The system employs a parallel-light shadowgraphic method that consists of a double-spark source at the focal point of a converging Fresnel lens, and a similar lens to focus the light into a camera. The system is activated by the projectile which, after penetrating the target, triggers a transducer whose pulse is fed to a delay unit. The delay unit in turn triggers the spark unit when the projectile is within the parallel-light field. The result is a shadowgraph of the projectile and the accompanying punch-out material in two positions. The distance between the two images on the photograph (corrected by a suitable magnification factor) divided by the spark time interval gives the average velocity of the projectile.

This system enables the measurement of residual velocity with an error of only 1 to 2 percent and, at the same time, permits the observation of size, shape, distribution of other particles, and distortion of the projectile.

1. High-speed photography
2. Ballistics
3. Photographic analysis
4. Impact shock
5. Velocity
6. Terminal ballistics
7. Projectile trajectories
8. Ballistic cameras
9. Shock waves

I. Title
II. Taneholtz, Stanley D.
III. Series

AD- Div. 24 Accession No. UNCLASSIFIED

U.S. Army Natick Laboratories, Natick, Mass. A PHOTO-OPTICAL SYSTEM FOR THE MEASUREMENT OF PROJECTILE VELOCITY by Stanley D. Tanenholtz. Oct 1965, 57 pp illus (Technical Report C&OM 1)

A photo-optical system has been developed for determining the velocity of a projectile after target penetration. This system provides a wide field of view and overcomes the difficulties introduced by light from the projectile-target impact and by the pretriggering of velocity-measuring transducers by particles broken from the target.

The system employs a parallel-light shadowgraphic method that consists of a double-spark source at the focal point of a converging Fresnel lens, and a similar lens to focus the light into a camera. The system is activated by the projectile which, after penetrating the target, triggers a transducer whose pulse is fed to a delay unit. The delay unit in turn triggers the spark unit when the projectile is within the parallel-light field. The result is a shadowgraph of the projectile and the accompanying punch-out material in two positions. The distance between the two images on the photograph (corrected by a suitable magnification factor) divided by the spark time interval gives the average velocity of the projectile.

This system enables the measurement of residual velocity with an error of only 1 to 2 percent and, at the same time, permit the observation of size, shape, distribution of other particles, and distortion of the projectile.

1. High-speed photography
2. Ballistics
3. Photographic analysis
4. Impact shock
5. Velocity
6. Terminal ballistics
7. Projectile trajectories
8. Ballistic cameras
9. Shock waves

I. Title
II. Taneholtz, Stanley D.
III. Series

AD- Div. 24 Accession No. UNCLASSIFIED

U.S. Army Natick Laboratories, Natick, Mass. A PHOTO-OPTICAL SYSTEM FOR THE MEASUREMENT OF PROJECTILE VELOCITY by Stanley D. Tanenholtz. Oct 1963, 57 pp illus (Technical Report C&OM 1)

A photo-optical system has been developed for determining the velocity of a projectile after target penetration. This system provides a wide field of view and overcomes the difficulties introduced by light from the projectile-target impact and by the pretriggering of velocity-measuring transducers by particles broken from the target.

The system employs a parallel-light shadowgraphic method that consists of a double-spark source at the focal point of a converging Fresnel lens, and a similar lens to focus the light into a camera. The system is activated by the projectile which, after penetrating the target, triggers a transducer whose pulse is fed to a delay unit. The delay unit in turn triggers the spark unit when the projectile is within the parallel-light field. The result is a shadowgraph of the projectile and the accompanying punch-out material in two positions. The distance between the two images on the photograph (corrected by a suitable magnification factor) divided by the spark time interval gives the average velocity of the projectile.

This system enables the measurement of residual velocity with an error of only 1 to 2 percent and, at the same time, permits the observation of size, shape, distribution of other particles, and distortion of the projectile.

1. High-speed photography
2. Ballistics
3. Photographic analysis
4. Impact shock
5. Velocity
6. Terminal ballistics
7. Projectile trajectories
8. Ballistic cameras
9. Shock waves

I. Title
II. Taneholtz, Stanley D.
III. Series

U. S. ARMY NATICK LABORATORIES
Natick, Massachusetts

CLOTHING & ORGANIC MATERIALS DIVISION

Technical Report
C&OM 1

A PHOTO-OPTICAL SYSTEM FOR THE MEASUREMENT OF PROJECTILE VELOCITY

Stanley D. Tanenholtz*
Materials Research Branch

*Now with Pioneering Research Division

Project Reference:
1X0-24401-A113

October 1963

FOREWORD

There has been a continuing need in ballistic studies for an accurate and reliable method of measuring velocities after target penetration. The system here described provides versatility as well as accuracy and reliability in projectile velocity measurement.

Inherent in this instrument, in addition to velocity measurement, is its ability to examine simultaneously many significant phenomena occuring during impact of a projectile with armor. It is therefore hoped that, through studies involving this instrument, much will be learned about the basic properties of materials under impact, which will, in turn, allow for the design of a superior, lightweight armor.

S. J. KENNEDY
Director
Clothing & Organic Materials Division

Approved:

DALE H. SIELING, Ph. D.
Scientific Director

MERRILL L. TRIBE
Brigadier General, USA
Commanding

CONTENTS

LIST OF FIGURES

LIST OF FIGURES (continued)

ABSTRACT

A photo-optical system has been developed for determining the velocity of a projectile after target penetration. This system provides a wide field of view and overcomes the difficulties introduced by light from the projectile-target impact and by the pretriggering of velocity-measuring transducers by particles broken from the target.

The system employs a parallel-light shadowgraphic method that consists of a double-spark source at the focal point of a converging Fresnel lens, and another similar lens to focus the light into a camera. The system is activated by the projectile which, after penetrating the target, triggers a transducer whose pulse is fed to a delay unit. The delay unit in turn triggers the spark unit when the projectile is within the parallel-light field. The result is a shadowgraph of the projectile and the accompanying punchout material in two positions. The distance between the two images on the photograph (corrected by a suitable magnification factor) divided by the spark time interval gives the average velocity of the projectile.

This system enables the measurement of residual velocity with an error of only 1 to 2 percent and, at the same time, permits the observation of size, shape, distribution of other particles, and distortion of the projectile.

A PHOTO-OPTICAL SYSTEM FOR THE MEASUREMENT OF PROJECTILE VELOCITY

1. Introduction

a. Review of techniques for measuring projectile velocity and observing high-speed phenomena

Accurate velocity measurement and observation of objects moving at high velocities have become increasingly important in gaining a better understanding of material properties. Difficulties involved in such measurements have been rapidly overcome, resulting in a wide variety of velocity-measuring techniques. Many of these find application in such diverse fields of research as ballistics and biology.

Velocity measurement techniques may be described in three broad classes: transducer, mechanical, and photographic.

1). Transducer techniques. One general example uses an electronic counter and two transducers. The transducers sense the approach or contact of a projectile. One transducer starts the counter and then, after the projectile has traveled a measured distance, the other transducer stops the counter. Since the distance between the start and stop positions is known, it is only necessary to read the counter and divide this time into the distance to obtain the average velocity between start and stop positions.

Transducers employ a variety of mechanisms. A photomultiplier tube has been used: a) in a multiple reflection system (16) to achieve a large field and increased sensitivity; b) with a long filament source in direct alignment (1); c) with a direct alignment source using lenses (1) to focus the light more efficiently and eliminate shock-wave effects; and d) in a system in which a projectile-punctured diaphragm allows light to pass into the photo-tube.

A continuous silver or aquadag grid (2) has been used as a cathode resistor in a thyratron circuit. Breaking the grid causes the tube to fire, resulting in a large-amplitude, sharp-output pulse.

A thin oriented polyester film or paper sheet, with a metallic coating on both sides, has been used in a "make" circuit (2) in which penetration of a missile completes the circuit, causing a thyratron to fire.

Magnetic coil (3) or toroidal transformer type transducers have been used to measure projectile velocities as well as for triggering other devices. A coil consists of a primary and secondary wound concentrically. With a direct current excitation voltage on the primary, a projectile passing through the coil will produce a voltage across the secondary.

Another transducer technique that has shown promise for measuring projectile velocity, requires only a single transducer and a frequency-change-to-voltage converter. The transducer in this case consists of a radio frequency oscillator. The rate of change of frequency, resulting from a metallic object passing through the coil (in the tank circuit), is proportional to the velocity of the object. A transducer of this type can also be used as a proximity device to trigger a counter.

An acoustic transducer technique has also shown promise for projectile-velocity measurement. This technique employs the acoustic pulse, generated by a projectile contacting a sheet of paper (which is transformed by the transducer into an electrical pulse), to start and stop a counter over a desired interval.

2). Mechanical techniques. An older velocity-measurement technique uses a ballistic pendulum (of large mass compared to the projectile) suspended in such a manner that the vertical rise on stopping the projectile is small compared to the length of the suspension. In this situation, the projectile velocity is essentially equal to a constant times the horizontal displacement of the pendulum.

A mechanical device employing rotating discs (10) has been used to measure projectile velocities. In this device, two paper discs are spaced at a measured distance and are rotated at the same constant angular velocity. A projectile penetrating these discs along a line parallel to the axis of rotation makes two holes angularly displaced from each other. From the angular velocity of the discs, their distance from each other, and the angular displacement between the holes, the projectile velocity may easily be calculated.

3). Photographic techniques. Photographic methods for observing high-speed events are numerous and well delineated in the literature. Only a few of these are applicable for routine projectile velocity measurements in a ballistic range, either because of cost or complexity of operation. However, many ingenious techniques have been developed for observing and quantitatively determining ballistic phenomena.

Various forms of high-speed, multiple-frame cameras are manufactured. Some of these use a continuous film feed and a rotating prism for framing (20), with framing speeds of 10 to 10,000 frames/sec. Others use a rotating drum for film transport (with the film around either the interior or the exterior periphery) and a rotating prism for framing (8), with framing speeds of approximately 200 to 25,000 frames/sec. Still others use a rotating mirror in a light lever arrangement to produce several single, short-duration photographs (8). The maximum framing rate of this type of camera is on the order of 10^6 frames/sec, with a shuttering speed of about 10^{-8} seconds.

Multiple flash light sources (7) and stroboscopes have been used to photograph high-speed events, to photograph changes in position on a single film, and to produce multiple frames with continuously moving film. The maximum flashing rate of one of the higher-speed stroboscopes is 300,000 flashes/sec (11). Millimicrosecond single sparks (9) are also available.

Image dissection cameras (13) have been used to obtain valuable data at maximum framing rates of 10^6 frames/sec. Systems based on this principle use scanned lenticular lenses and gratings to dissect an image.

A slit camera (4) has been used with much success for hypervelocity measurements. This method involves the projection of the projectile image on a narrow slit whence it is focused on a rapidly moving film.

Short-duration (in the order of 10^{-8} sec) multiple frames are available by means of an electronic image converter (15).

A novel multiple-spark source of short duration (0.1 microsecond) and high intensity has been developed for high-velocity shock-tube photography (14). The systems consist of capacitors with contiguous spark gaps arranged in an optical system so that the image of all sources appears at a single point.

Magneto-optic (12) and electro-optic (16) shutters are used in high-speed cameras with shutter speeds of 0.8×10^{-6} sec and 0.005×10^{-6} sec respectively. These shutters, however, have the disadvantage of small viewing angles.

b. Utility of the photo-optical system

Some of the previously-mentioned techniques require much time, expense, and effort in data reduction; other techniques are not sufficiently accurate for our purposes. We require a system that is versatile and yet sufficiently accurate to distinguish differences in material properties in a ballistic impact.

The photo-optical system we have developed overcomes many of the difficulties of previously mentioned techniques. It is used to measure: a) the ballistic limit of a material in terms of the projectile striking velocity required for penetration, and b) the projectile velocity after penetration of the target. The latter is its primary use since simpler systems can be satisfactorily employed for determining striking velocity. For measuring the residual velocity of projectiles that have penetrated metal plates or many plastic sheets, the photo-optical system overcomes the difficulties caused by "punchout" that affect most transducer systems. "Punchout" refers to any fragmentary material broken from the target by the direct force of the projectile or by the tensile forces caused by shock waves reflected from the rear surface of the target. The nature and quantity of the punchout depends on the physical properties of the material and the projectile velocity. For example, with acrylic sheet targets, at velocities of from 1000 to 3000 ft/sec, there is a considerable amount of jagged punchout material of varying sizes, whereas in thin aluminum targets in the same velocity range, the punchout takes the form of a small piece of metal with a diameter approximately equal to that of the projectile. The punchout (Figs. 1 and 2) may precede and trigger the velocity-measuring system, thereby giving an erroneous reading of time on the counter. Such uncertainty made it necessary that we consider methods by which we could observe the projectile.

Figure 1. Major punchout preceeding 17-grain fragment simulator after penetrating a titanium alloy sheet. Impact velocity: 2004 ft/sec (double exposure).

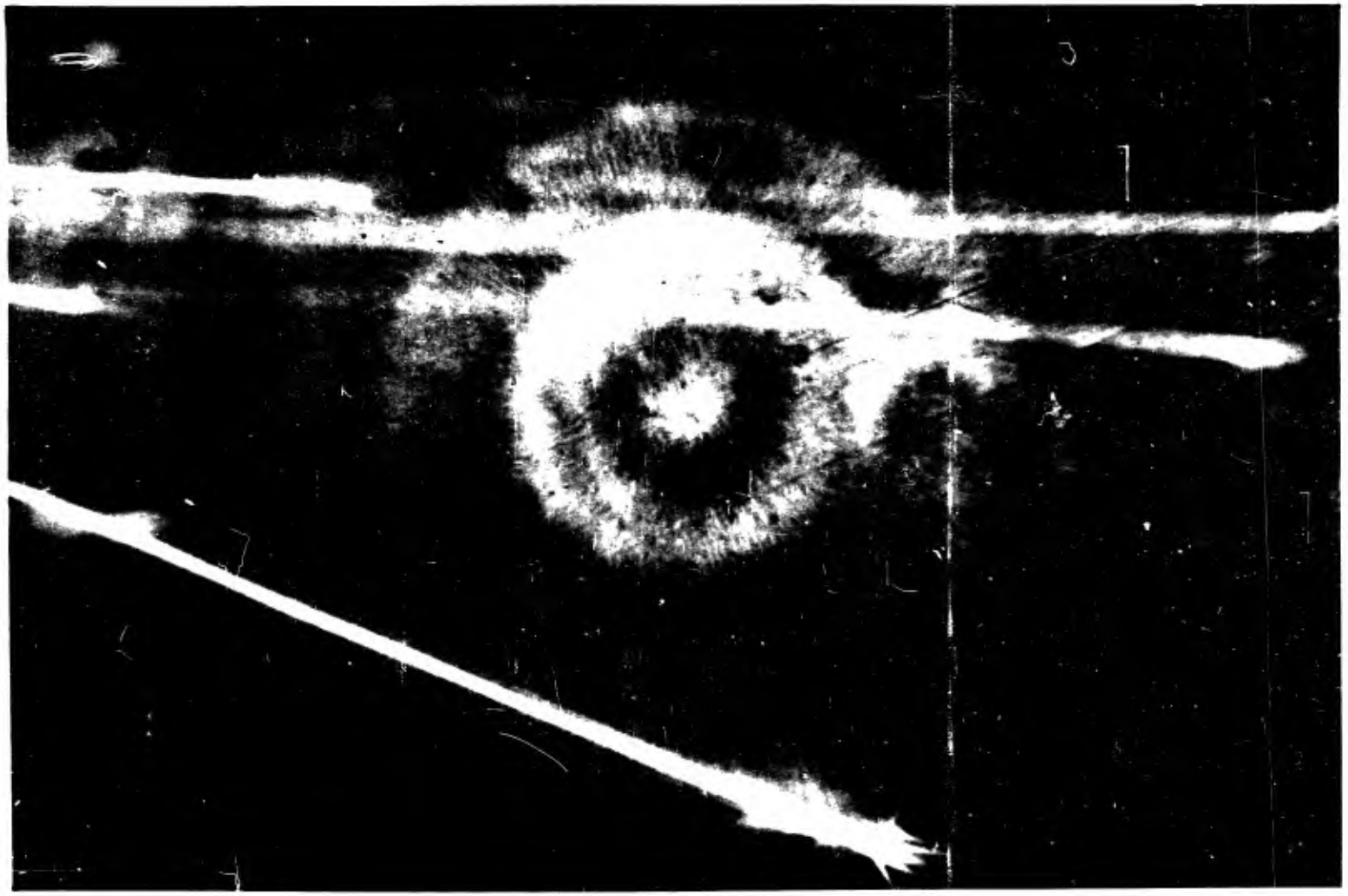

Figure 2. Major punchout <u>following</u> 17-grain fragment simulator after penetrating a titanium alloy sheet. Impact velocity: 2893 ft/sec (double exposure).

The simplicity of a spark-shadowgraph system led us to develop projectile velocity measurements and observation techniques along that line.

Previous spark-shadowgraphic systems used by us had the disadvantages of narrow field (due either to the use of small lenses or to a non-parallel light field), extreme variation of magnification with small changes in object distance, and impact light obliterating the photographic image. The photo-optical system that will be described here has none of these disadvantages.

2. Theory

a. Basic system

In theory, we have a point source of light that can be triggered to flash twice over a desired time interval and initiated when the projectile is in the light field (Fig. 3). This point source is placed at the focus of a large converging lens, thereby producing a parallel-light field.

To focus the total field into a camera, we must place another converging lens of the same size parallel to the first and on the same optical axis, with sufficient space between these two lenses to allow the projectile and other particles to pass without injuring the lenses. The second lens focuses anything within this field. To obtain a full view of the lens field, the image of the field at the camera must be smaller than the entrance pupil. Increasing the size of the lens would, of course, increase the size of the parallel-light field.

The primary advantages of a parallel-light field are: a) a large field of view (equal to lens diameter), and b) constant magnification of an object anywhere in the parallel-light field.

The operation of the system depicted by Figure 3 starts with the firing of a projectile through an initial measuring system (to determine striking velocity) before impacting the target. Assuming a metal target, the projectile, on penetrating the target, will be both preceded and followed by particles of metal from the target (see punchout illustrated in Figs. 1 and 2). After the target has been penetrated, either a punchout particle or the projectile will trigger a photoelectric light screen (or some other triggering transducer). The pulse from this transducer is then delayed until the projectile is within the lens field, after which time the spark gap is activated (a second spark follows the first by a pre-selected time interval), and two pictures of the projectile and punchout material are taken. We have some latitude in timing, since both the spark time interval and the delay time are variable and the lens field is large. The result is a shadowgraph of the projectile and the punchout material in two positions. The distance between the two photographic images of the projectile (corrected by a suitable magnification factor), divided by the time interval over which the two images were produced (neglecting air drag, which is a small consideration over the distance involved), gives the average projectile velocity.

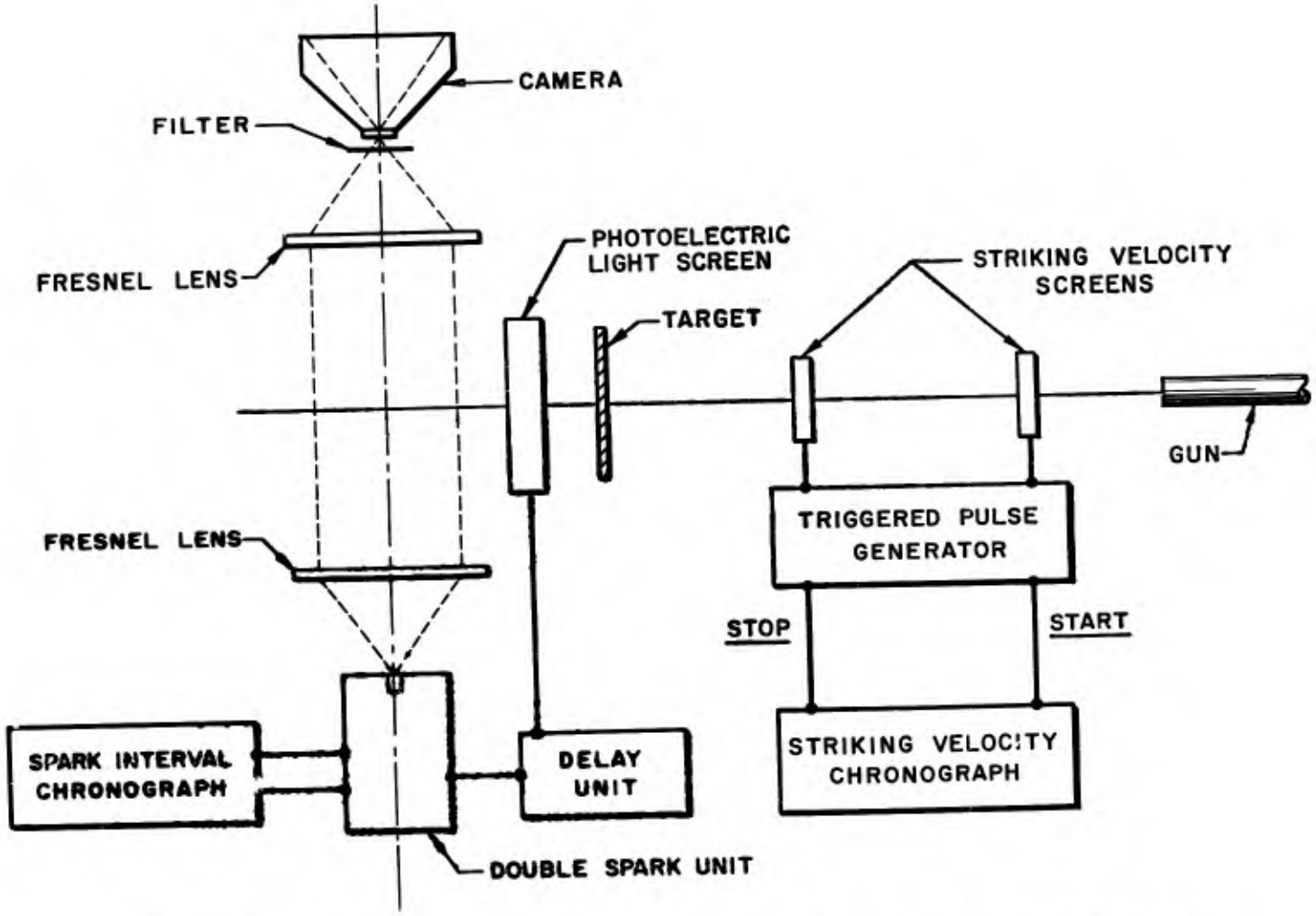

Figure 3. Schematic diagram of the photo-optical velocity-measurement system.

b. Lenses

In the photo-optical system with well-collimated light, the rays, and any projected image produced by an object between the lenses blocking out a portion of the light field, are converged to the focal point of the second lens at the surface of the camera lens and are thence imaged on the film. Since in the parallel-light field there are no rays (except for dispersion at the edges of the object) that are deflected through the center of the second lens, the magnification (given by the ratio of image to object size) will not change with varying object distance within the parallel-light field. Also, any light that is produced within the field, such as from glowing particles of the target material due to impact, will be dispersed by the second lens (out of focus relative to the camera), since the main flash is a broad source and the glowing particles of target material are, in general, out of focus.

From elementary Gaussian optics, we have for our system:

$$x_i = \frac{f x}{f - x}$$

where:

f = focal length of lens
x_i = image distance
x = object distance

If: $x = f$

then: $x_i = \frac{f^2}{0} = \infty$

Therefore a light source small enough to be placed accurately at the focal point of a converging lens will produce parallel light. Of course, the quality of parallel light is influenced by the degree of spherical aberration in the lens, i.e., the degree to which all parts of a positive lens converge parallel light to a single focal point.

Spherical aberration and curvature of field, which might produce out-of-focus or distorted images at the edges of the field, tend to limit the useful field size. The focal lengths of the field lens and camera lens, as well as the diameter of the camera entrance pupil, will also limit the field of view. To a large extent, spherical aberration and curvature of field may be corrected by an appropriate stop. Also, spherical aberration may be decreased by the use of long focal-length lenses.

Spherical aberration may occur laterally and longitudinally and is defined by the following:

$$\text{Lateral spherical aberration} = \frac{1}{S_h} - \frac{1}{S}$$

where S_h = image distance for an oblique ray traversing the lens at a distance h from the axis.
S = image distance for paraxial rays

Longitudinal spherical aberration = $S - S_h = (S)(S_h)$ (lateral spherical aberration)

Another aberration of considerable significance in our system is distortion, as indicated by a variation in magnification across the image. Although some correction for curvature of field and spherical aberration may be made by means of a stop, nonlinear distortion will still be present if it is caused by nonlinear magnification inherent in the lenses.

The resolution of the system involves two terms, the optical resolution and the film resolution. The optical resolution may be defined by considering the Rayleigh criterion as a limit of resolution. Then we have:

$$\alpha = \frac{\lambda}{a} \quad , \text{ or } d = f\frac{\lambda}{a}$$

where:
d = resolution in terms of resolved lines
α = minimum angle of resolution
a = size of the aperture
f = focal length of the lens
λ = wave length of light used (essentially blue for our spark source).

The limiting aperture of the system is ordinarily that of the camera lens.

The "film resolution" is defined as the minimum number of resolved lines at a given lens-to-object distance. In order to compare the resolution using the camera alone, we must make the comparison at the same magnification.

Image magnification may easily be accomplished (although with decreased light on the film and decreased field) by the use of a short focal-length camera lens, or the field size may be increased by the use of a long focal-length lens (Fig. 4).

Converging Fresnel lenses may be used for the field lenses required in our system. They consist of plastic sheets on one side of which concentric, prism-shaped, circular grooves have been cut. In some instances, Fresnel lenses are manufactured with the grooves in the form of a continuous spiral. The spiral, however, is quite closely concentric. Fresnel lenses may be obtained in sizes varying from approximately 1 inch to approximately 20 inches in diameter, and with focal lengths varying from approximately 1 to 40 inches. Focal length is determined by the groove angles. The focal length of any Fresnel lens may be halved by using two identical lenses face to face. The focal length (F) of any lens may be varied by using the following well-known formula:

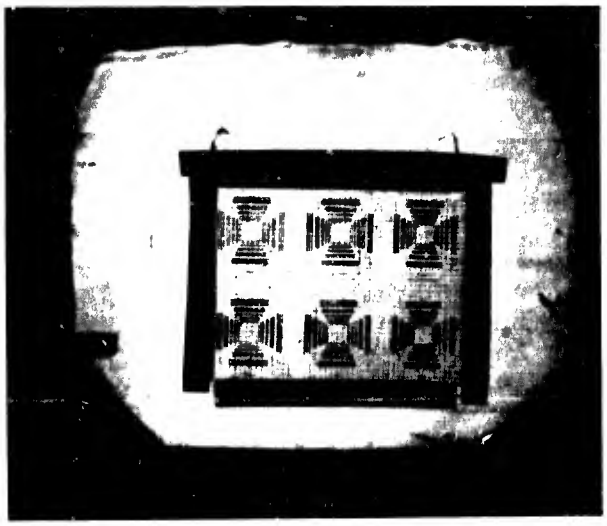

a. Resolution chart

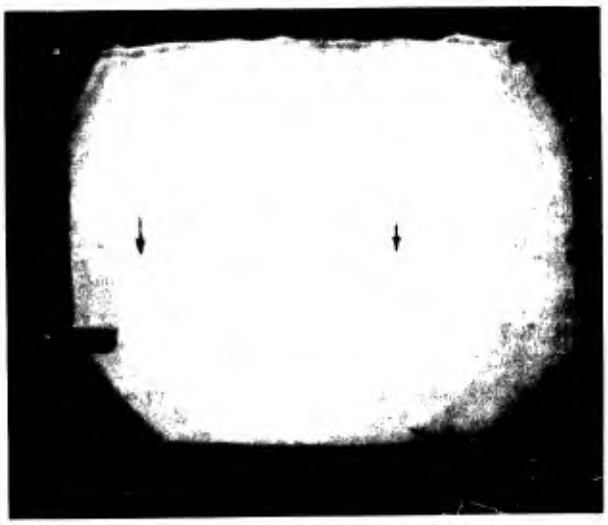

b. Projectile in flight at two positions on the film.

Figure 4. Total light field using a 10-inch focal-length lens.

$$\text{Lateral spherical aberration} = \frac{1}{S_h} - \frac{1}{S}$$

where S_h = image distance for an oblique ray traversing the lens at a distance h from the axis.
S = image distance for paraxial rays

Longitudinal spherical aberration = $S - S_h = (S)(S_h)$ (lateral spherical aberration)

Another aberration of considerable significance in our system is distortion, as indicated by a variation in magnification across the image. Although some correction for curvature of field and spherical aberration may be made by means of a stop, nonlinear distortion will still be present if it is caused by nonlinear magnification inherent in the lenses.

The resolution of the system involves two terms, the optical resolution and the film resolution. The optical resolution may be defined by considering the Rayleigh criterion as a limit of resolution. Then we have:

$$\alpha = \frac{\lambda}{a} \quad , \text{ or } \quad d = f\frac{\lambda}{a}$$

where:
d = resolution in terms of resolved lines
α = minimum angle of resolution
a = size of the aperture
f = focal length of the lens
λ = wave length of light used (essentially blue for our spark source).

The limiting aperture of the system is ordinarily that of the camera lens.

The "film resolution" is defined as the minimum number of resolved lines at a given lens-to-object distance. In order to compare the resolution using the camera alone, we must make the comparison at the same magnification.

Image magnification may easily be accomplished (although with decreased light on the film and decreased field) by the use of a short focal-length camera lens, or the field size may be increased by the use of a long focal-length lens (Fig. 4).

Converging Fresnel lenses may be used for the field lenses required in our system. They consist of plastic sheets on one side of which concentric, prism-shaped, circular grooves have been cut. In some instances, Fresnel lenses are manufactured with the grooves in the form of a continuous spiral. The spiral, however, is quite closely concentric. Fresnel lenses may be obtained in sizes varying from approximately 1 inch to approximately 20 inches in diameter, and with focal lengths varying from approximately 1 to 40 inches. Focal length is determined by the groove angles. The focal length of any Fresnel lens may be halved by using two identical lenses face to face. The focal length (F) of any lens may be varied by using the following well-known formula:

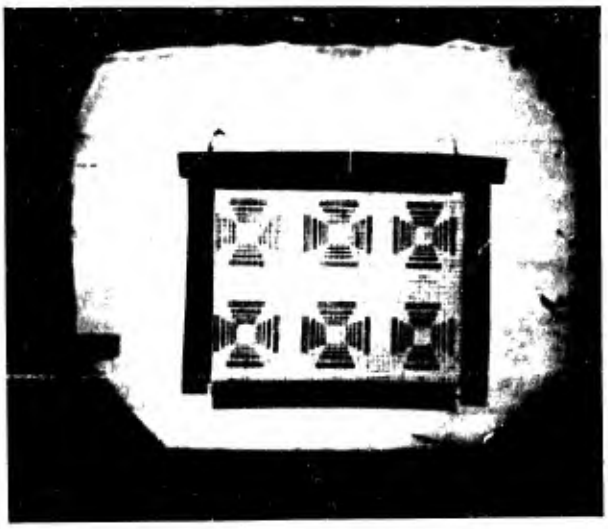

a. Resolution chart

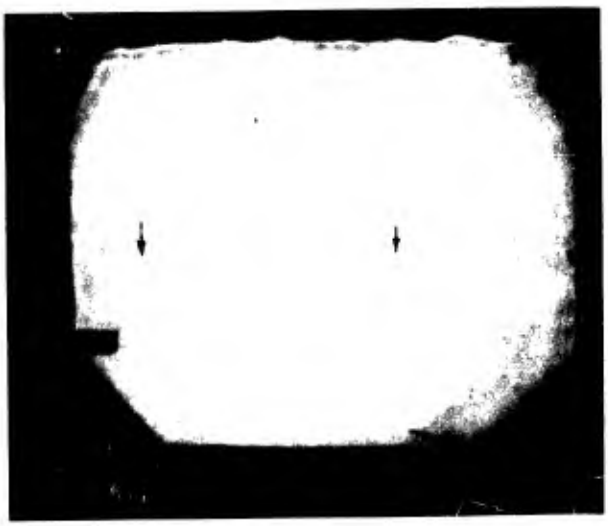

b. Projectile in flight at two positions on the film.

Figure 4. Total light field using a 10-inch focal-length lens.

$$F = \frac{f_1 f_2}{f_1 + f_2 - d}$$

where f_1, f_2 and d are, respectively, the focal lengths of the two lenses and their separation.

Since the focus of rays in individual portions of the lens may be varied by suitable shape and guidance of the cutting tool, spherical aberration may be completely corrected. The spherical aberration of a Fresnel lens, as in ground lenses, is different for light incident on either of its two surfaces. In the case of the Fresnel lenses we use, spherical aberration is least for light incident on the grooved surface. The apparent decrease in luminance in various zones of the Fresnel lenses results from surface discontinuities and is influenced by the angle of incident light and the side on which it is incident (6). Misalignment may result not only in increased off-axis aberrations but also in objectionable moiré pattern. The resolving power of a Fresnel lens has been considered as that of a square aperture with a width equal to the width of one groove.

c. Spark light source

The spark unit (Fig. 5) consists essentially of a capacitor for storing electrical energy and an air gap through which the energy is discharged, producing a small high-intensity light source.

The circuit operation can be described by the well-known differential equation (17) for a resistance, inductance, and capacitance in series and activated by a direct current source. The equation of the network is:

$$L\frac{d^2 i}{dt^2} + R\frac{di}{dt} + \frac{i}{C} = 0 \qquad (1)$$

The solution of Equation (1) for $(\frac{R}{2L})^2 < \frac{1}{LC}$ is:

$$i = \frac{V}{L\sqrt{\frac{1}{LC} - (\frac{R}{2L})^2}}\, e^{-\frac{Rt}{2L}} \sin\sqrt{\frac{1}{LC} - (\frac{R}{2L})^2}\, t \quad \text{and:} \quad f = \frac{1}{2\pi}\sqrt{\frac{1}{LC} - (\frac{R}{2L})^2}$$

where:

V = applied voltage (volts)
L = inductance (henries)
C = capacitance (farads)
R = resistance (ohms)
t = time (secs)
i = current (amps)
f = frequency of oscillation (cycles/sec)

If R is negligibly small, we have essentially:

$$i = V\sqrt{\frac{C}{L}}\, \sin \omega t$$

where:

$$f = \frac{1}{2\pi}\sqrt{\frac{1}{LC}}, \quad \omega = 2\pi f$$

In order to achieve as short a spark duration as possible (for minimum image smear), such oscillatory effects as described by the above equations must be diminished. We must therefore consider the case for which we have minimum oscillation (i.e., critical damping).

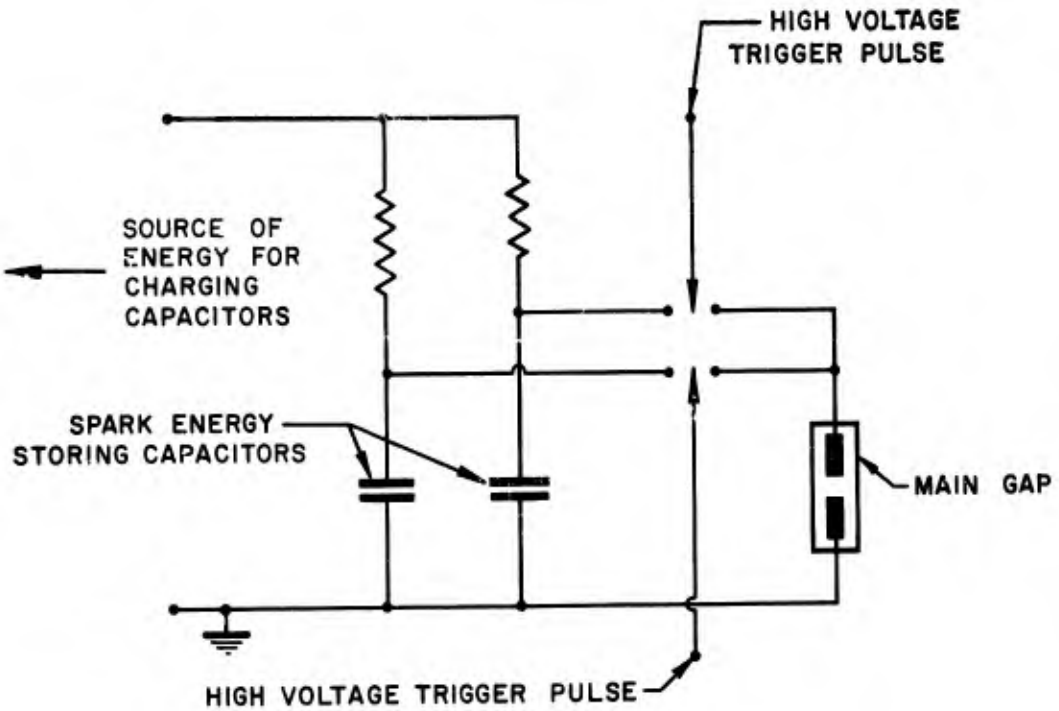

Figure 5. Basic spark unit diagram

The solution of Equation (1) for this case, when: $\left(\frac{R}{2L}\right)^2 = \frac{1}{LC}$

is: $i = \frac{V t e^{-Rt/2L}}{L}$ (2)

where the decay time (τ) of the circuit is: $\tau = \frac{2L}{R}$

The desired result is achieved by letting:

$$R = 2\sqrt{\frac{L}{C}} \quad \text{or} \quad C = \frac{4L}{R^2}$$

where, for any desired spark energy (E) and voltage (V): $C = \frac{2E}{V^2}$

Therefore, in order to achieve a high-energy spark (for good image contrast with background) and yet a short spark time (for minimum image smear), a compromise has to be made. Where there is extreme target flash, it would be advantageous to allow a long decay time with resulting increased spark energy.

3. Equipment

a. Optical bench

The photo-optical system (Fig. 6) was set up in the form of an optical bench, which consists essentially of a spark gap, two parallel Fresnel lenses, and a Speed-Graphic camera with a Polaroid back (see also Fig. 3). The equipment is aligned in the order described, and all components are centered as nearly as possible along one axis passing through the center of the lenses. The associated electronic counters and delay unit are arranged in convenient locations near the optical bench. The photo-optical system is mounted perpendicular to the line of fire from the gun. The line of fire passes through the striking velocity screens and target, and is centered between the two lenses. The optical bench (Fig. 6) can be extended from 9 to 16 feet and may be raised from a 3-foot level to 5 feet by the supporting hydraulic table.

Figure 7 shows the gun mount, delay unit, and the striking velocity counters.

b. Spark unit

The spark unit is a commercial double-flash type unit. A time interval between sparks of from 0 to 100 microseconds can be obtained with this instrument. We have extended this range to approximately 1000 microseconds (in order to increase the base line distance between projectile images at lower velocities) by inserting a capacitor in parallel and a resistor in series with those already in the delay circuit of the instrument. Switches across the resistor and in series with the capacitor allow them to be removed from the circuit when necessary.

The duration of the spark and its intensity are interdependent, as indicated by Equation (2), page 12. We found it advantageous to use additional plug-in capacitors to achieve increased spark intensity. The maximum capacitance that we used in a single spark discharge was 0.015 microfarads. This resulted in negligible image blur, as is evident in Figures 1 and 2. The duration of the spark (down one-third of maximum intensity) was approximately 0.4 microseconds with 0.005 microfarad capacitance and 1 microsecond with 0.015 microfarad capacitance. The arrangement of the plug-in capacitors is shown in Figure 8.

An extra spark gap, detached from the unit, has been constructed for those situations where space will not permit the use of the complete spark unit. The rise and decay times of the light pulse from this extra spark gap were approximately 1 and 2 microseconds, respectively. Lead lengths were 2 feet and it appears to make little difference in rise and decay times whether the leads were close together or separated.

Two basic methods have been used to trigger the spark. These are illustrated in Figure 9. The upper diagram in Figure 9 illustrates a method in which the projectile or punchout material on the exit side of

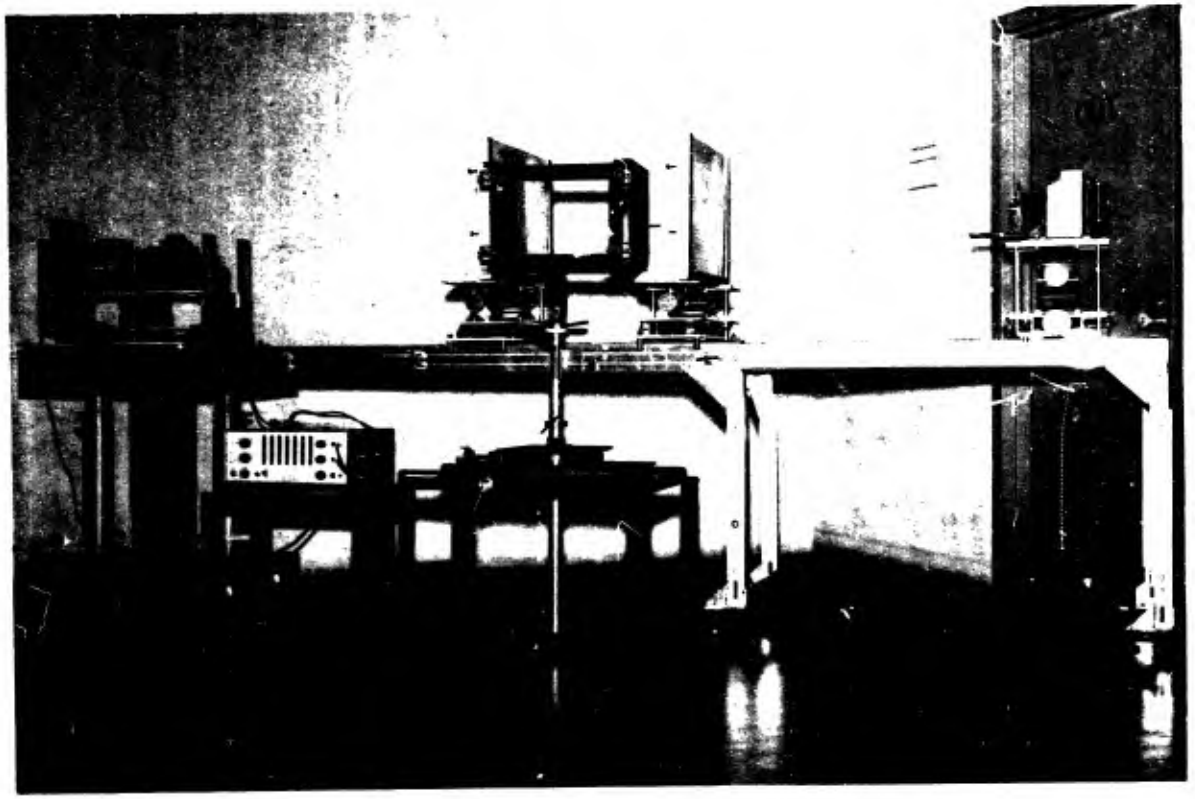

Figure 6. Photo-optical system (side view) with complete target-holder assembly.

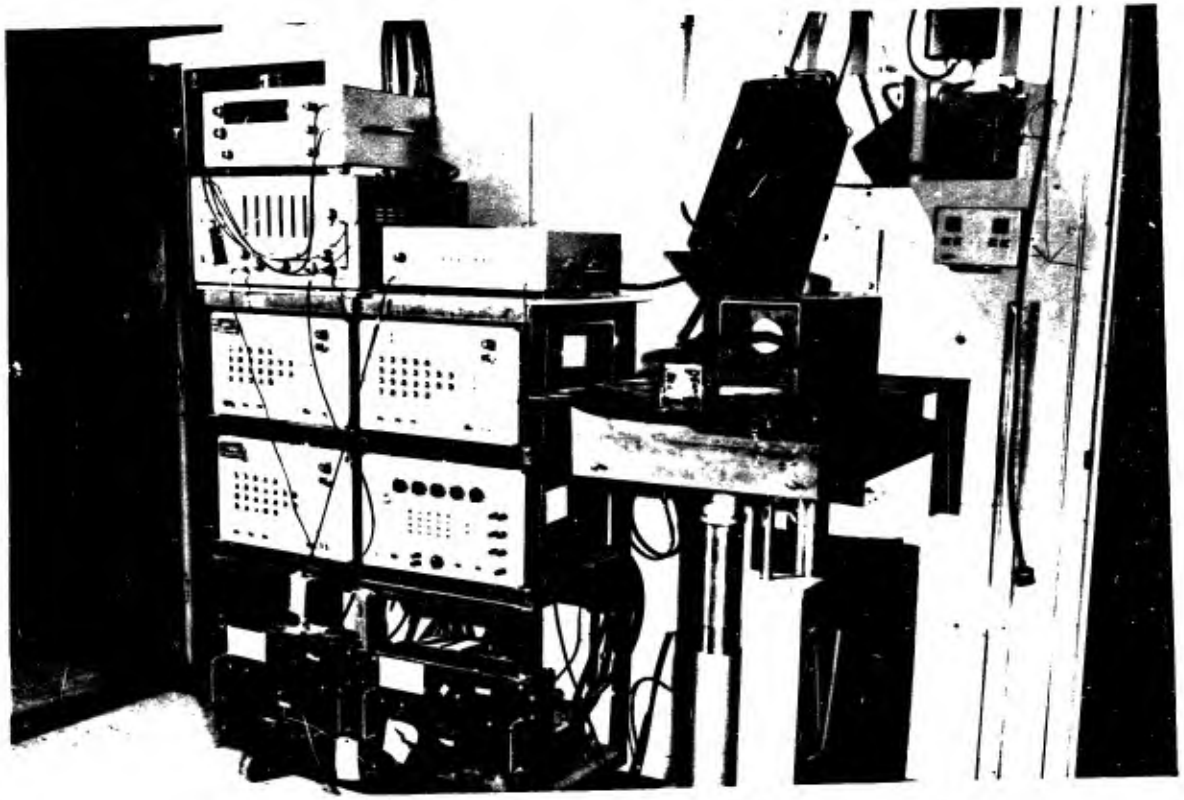

Figure 7. Gun and auxiliary electronic equipment.

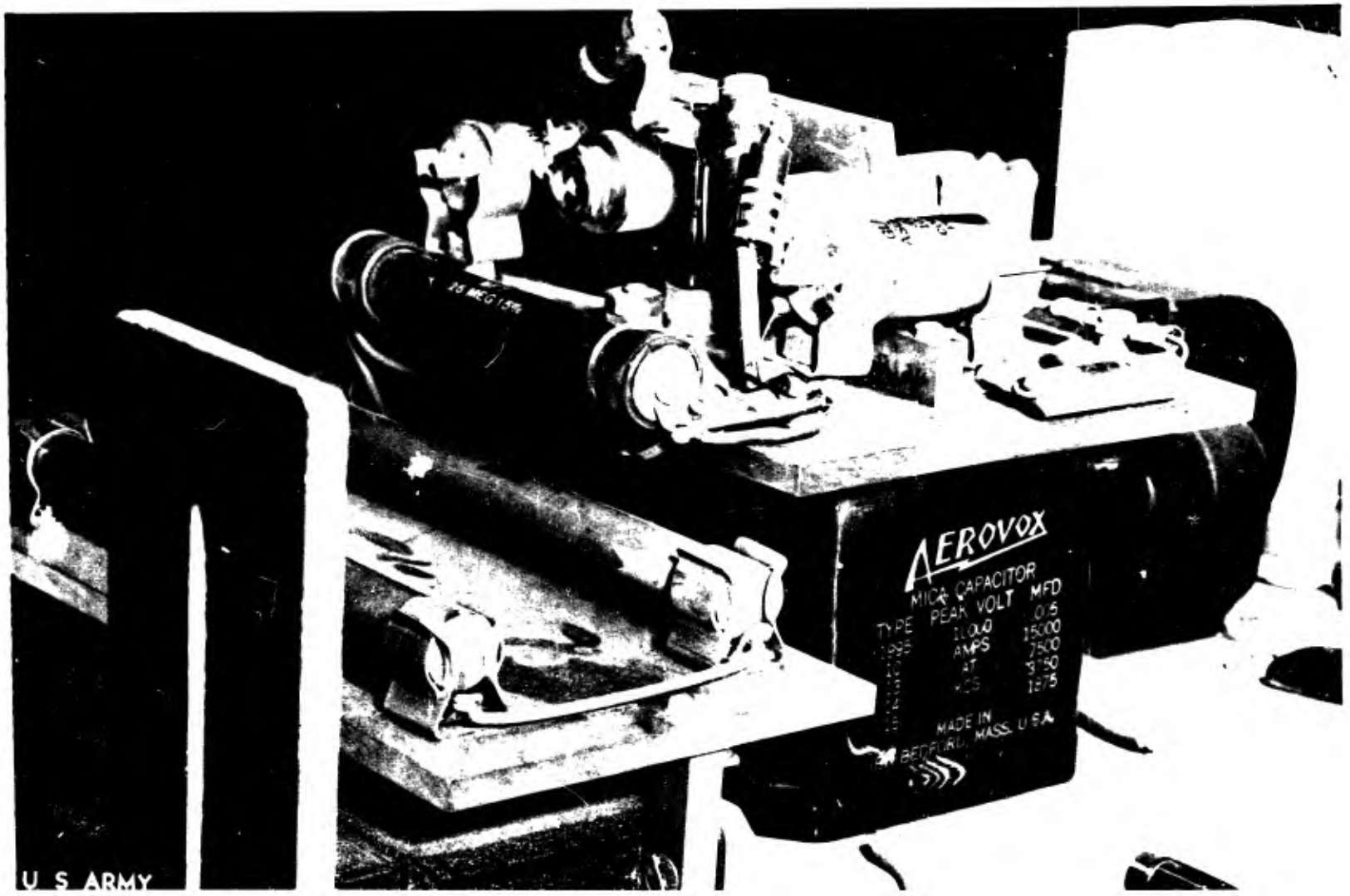

Figure 8. Spark unit, with additional capacitors clamped in position.

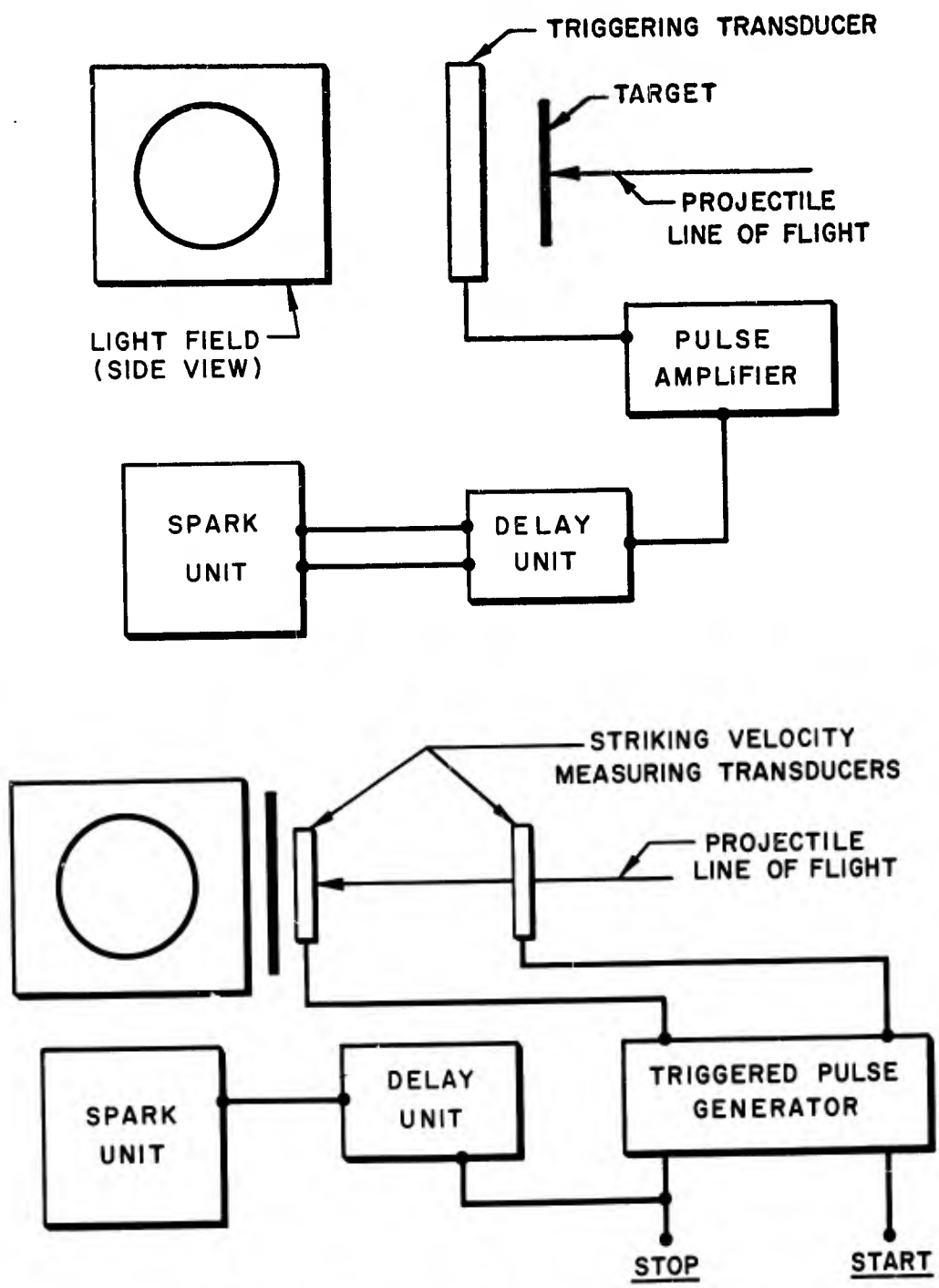

Figure 9. Schematic diagrams of two spark-triggering methods.

the target triggers a transducer (which may be a light screen, "make" or "break" circuit, magnetic coil, or radio frequency coil). The pulse from this transducer is delayed until the projectile has had sufficient time to enter the light field, at which time the double-spark unit is triggered. The result is a shadowgraph of the projectile in two positions. When this method is used with a transducer that does not distinguish between projectile and punchout, occasionally (as a result of premature triggering of the spark unit) one or both of the projectile images may not appear on the film. This premature triggering is caused at velocities approaching the ballistic limit of the material by the punchout preceding the projectile (Fig. 2) by a sizeable and unpredictable distance.

The lower diagram in Figure 9 illustrates a method that is used when the target is either in or close to the light field. The pulse produced by the projectile triggering the stop transducer of the striking-velocity-measurement system is sent simultaneously to the counter and to the delay unit. The delay pulse then triggers the spark unit. There is no problem in this method of the punchout pretriggering the transducer. However, it requires estimation of the projectile's residual velocity in order to properly set the delay. This involves some trial and error. However, once two images of the projectile, and thence the residual velocity, are obtained at a particular striking velocity, it becomes a relatively simple operation to "capture" both images at other striking velocities.

c. Fresnel lenses

The Fresnel lenses that we are now using are 17 by 22 inches and are corrected for spherical aberration. These particular lenses were selected because they were the largest available at a low price. They replaced 14-inch-diameter overcorrected lenses. The 17- by 22-inch lenses with a focal length of 40 inches produced the best parallel light field, although their f number was smaller than that of the 12- and 14-inch focal length lenses tried. These lenses are shown in Figure 10.

d. Camera and filters

In our system we use a Speed-Graphic camera (with $f/4.5$, 5-inch focal length and $f/5.6$, 10-inch focal length interchangeable lenses) equipped with several demountable backs, solenoid shutter release, and filter.

The backs are all mountable with the standard graphlock fixture. These include a Polaroid 3-1/4 by 4-1/4 inch roll film back, a Polaroid 4- by 5-inch film back, a spring back for cut-film holders, and a ground glass focusing screen for each film size.

The production of extraneous light, due to the impact of projectiles on metal targets and the resultant glowing metal particles, caused difficulty in recording the projectile images, especially at the higher veloci-

Figure 10. Fresnel lenses: 12-inch focal length
40-inch focal length
14-inch focal length

ties (Fig. 11). A variety of filters were used to minimize this, depending on the type of film used and the lighting involved. The Kodak C5 No. 47 blue filter, and Corning 5113 and 5970 filters used with types 47 and 44 Polaroid films will eliminate by their color much of the light due to target impact flash. (The impact flash is predominantly in the red-yellow region, whereas the spark flash has strong lines in the blue, green, and violet regions.) Moreover, these filters also decrease the impact light to a point where the spark light becomes more effective in making an exposure. The Corning filters cut off more sharply in the blue and violet, thus attenuating the background target flash substantially more than the Kodak C5 No. 47 blue filter. The blue filter decreased the contrast somewhat but had no noticeable effect on the resolution.

Polarizing filters have been found useful in limiting target flash and thereby making the spark flash more effective without appreciably impairing the spectral resolution of the system. The use of such filters would be called for when making true color photographs of flash or color Schlieren phenomena.

e. Film

A variety of film is available for use in our system. Selection of a specific type is dependent on spark-source intensity and target-impact flash. The spark-source intensity may be adjusted so that, when used with the proper filter and film, it will produce the desired latitude (we may adjust the intensity to that portion of the film density-exposure curve which has maximum slope, i.e., maximum contrast). Therefore, if it is necessary to maintain a short spark time and a small spark source (thereby limiting the spark intensity), we may use a film having a suitable (in our case high) gamma value (contrast), and yet be sufficiently sensitive to record the image. It is necessary to take into consideration reciprocity failure, since it has been noted (5) that the faster films generally exhibit a lower gamma, as exposure time is reduced from 10^{-3} through 10^{-6} second, without loss in film speed. The slower films, however, exhibit considerable loss in film speed with little change in gamma. This indicates that we should use a maximum intensity spark source (without a filter) when using a low-speed film to obtain a high gamma.

In order to increase the speed of data reduction, Polaroid films have been used almost exclusively in our laboratory. Higher contrast, moderate speeds (A.S.A. 200) are available with types 52 and 53 (these are 4 x 5 in), with the type 53 having a reclaimable negative. When a larger base line is desired, these 4- by 5-inch films are useful. Type 42 (A.S.A. 200, 3-1/4 x 4-1/4 in) and type 46L (A.S.A. 400, 3-1/4 x 4-1/4 in lantern slide type) films have been used to advantage in defining small projectiles. Type 46L has also been used to achieve high contrast where extreme target flash is encountered. For general purposes, type 47 (A.S.A. 3000, 3-1/4 x 4-1/4 in) and type 44 (A.S.A. 400, 3-1/4 x 4-1/4 in) have been successfully used. It has been found, however, that type 47 film does not have sufficient latitude to be used without a filter in our system (the image is washed out). The newer high-speed, high-contrast type 410 film might be of considerable advantage in resolving

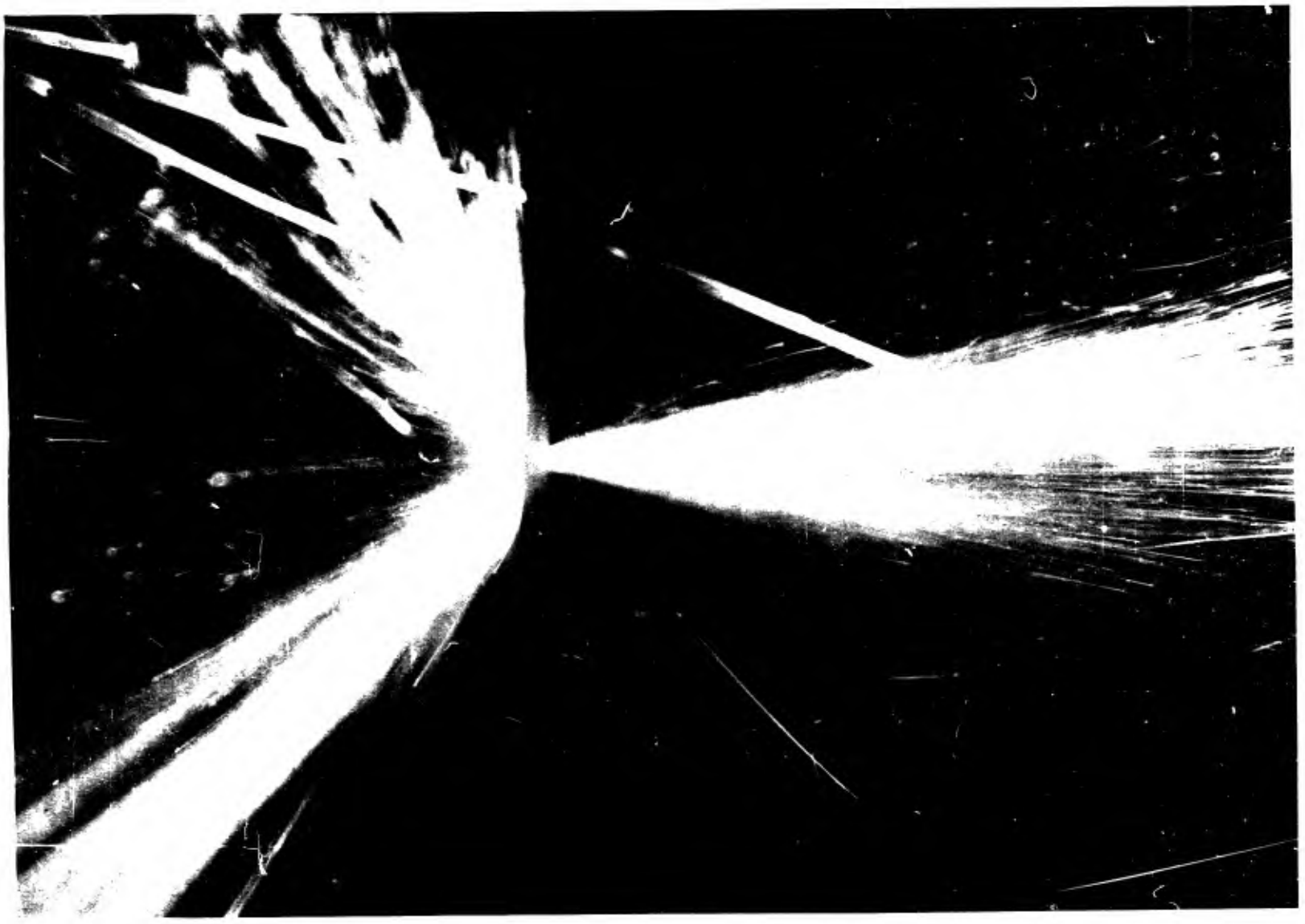

Figure 11. Impact flash

projectiles in the target flash.

f. Use of targets within parallel light field

There is considerable advantage in placing the materials to be impacted within the parallel-light field. This, in essence, eliminates the necessity for drag corrections. Another advantage of placing the target within the light field is that the projectile and target are seen simultaneously. We may therefore observe projectile-target interactions at the same time that we are measuring projectile velocity.

The target holder construction is seen in Figure 6. This holder allows lateral movements in two directions by means of rack and pinion gears at the base, and vertically (a distance of approximately 8 inches), by means of a screw. A gross adjustment also allows a vertical movement of several feet.

g. Electronic counters and delay units

We have used 1.6-megacycle counters for some time with a fair measure of reliability. These counters have an uncertainty of one count (0.6 microsecond) plus that of master oscillator stability (which amounts to an uncertainty of approximately 1 microsecond). With the acquisition of 10-megacycle transistorized counters, the accuracy and reliability of our time-interval measurement has increased, since the 10-megacycle counter has an uncertainty of only 10^{-7} microsecond plus that of its stability (which is one part in 10^{-7}).

We have also replaced a 100-kilocycle delay unit with a transistorized 1-megacycle unit. This will allow us to adjust our delays to within 1 microsecond.

4. Operational Procedures

a. Setting up

The first step in setting up the system is to try to eliminate, as nearly as possible, the effects of off-axis aberrations by aligning the components as accurately as possible. Alignment of the components along the optical axis is accomplished by a jig consisting of a stand with an attached pointer. The pointer is a rod, 10 inches long, held in a fixed level position perpendicular to the ways of the optical bench and at the height of the projectile line of flight. The jig is first moved close to the spark unit. The spark unit is then adjusted so that the main gap is horizontally and vertically in line with the pointer. The jig is then moved to the collimating Fresnel lens and its center aligned with the pointer. The other components are similarly aligned with the pointer and therefore with each other. It is then an easy matter to make the system perpendicular to the projectile flight.

The next step is to make certain that the light field between the

two Fresnel lenses consists of parallel light (or as nearly parallel as possible). This is accomplished by setting the point source at the calculated focal point of the first Fresnel lens and moving a measured block across the field, then determining any change in projected image size on the second Fresnel lens surface. (It should not change if we have parallel light.) The spark gap to lens distance is then adjusted to compensate for any changes. Even after adjustment, the light is not perfectly parallel, but is as nearly so as we can make it. We can eliminate much aberration by proper alignment but some spherical aberration and pincushion distortion remains.

Finally, the camera is moved along the optical axis (toward the second Fresnel lens) of the system until the smallest focal spot of the light source appears on the camera lens surface. The camera focus is then adjusted for maximum image resolution. All adjustments are made with the double-spark unit set to fire continuously.

The system may be set up for measuring projectile velocities as described, or for various methods of high-speed observation of projectiles or target deflection (e.g., reflection from a "scotchlite" screen, and direct shadowgraph by placing a film holder parallel to and close to the line of fire). Its construction is such that individual units have maximum versatility of movement and yet are rigid when locked in position (Figs 12, 13, and 14).

Figure 12. Film holder for direct shadowgraph; 3-inch target frame; and 11- x 12-inch target frame (from left to right)

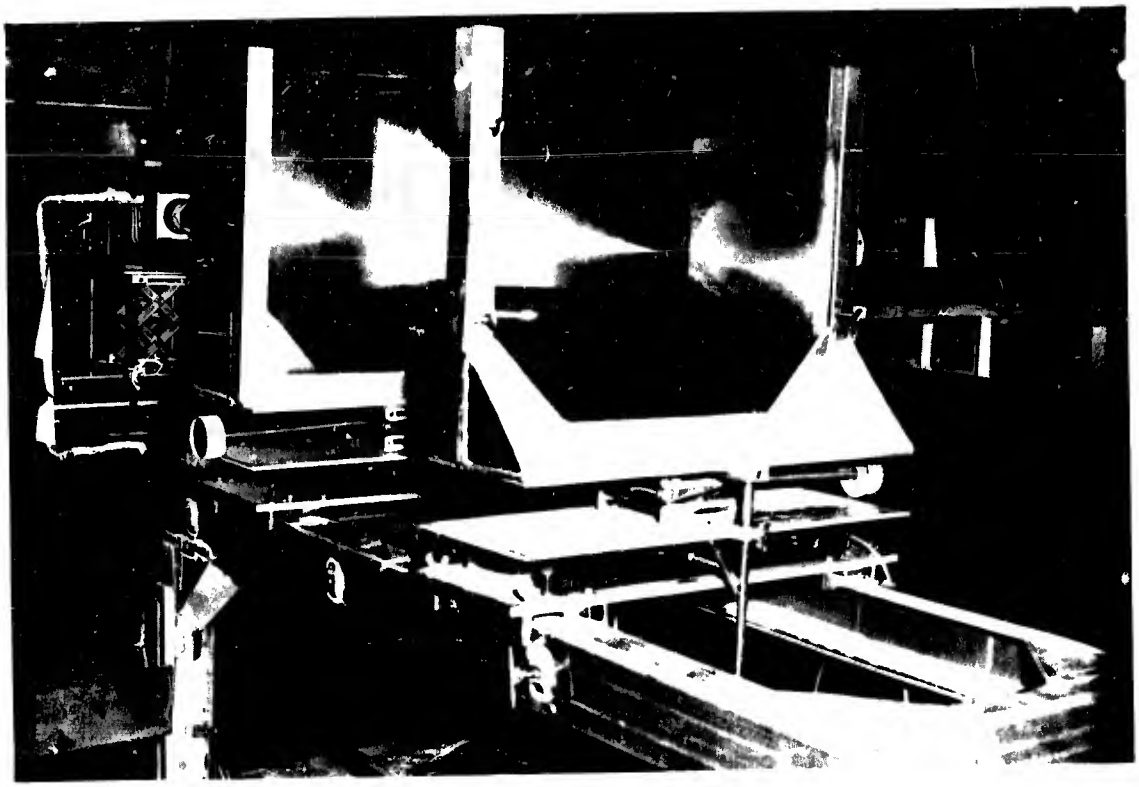

Figure 13. Photo-optical system from spark unit end.

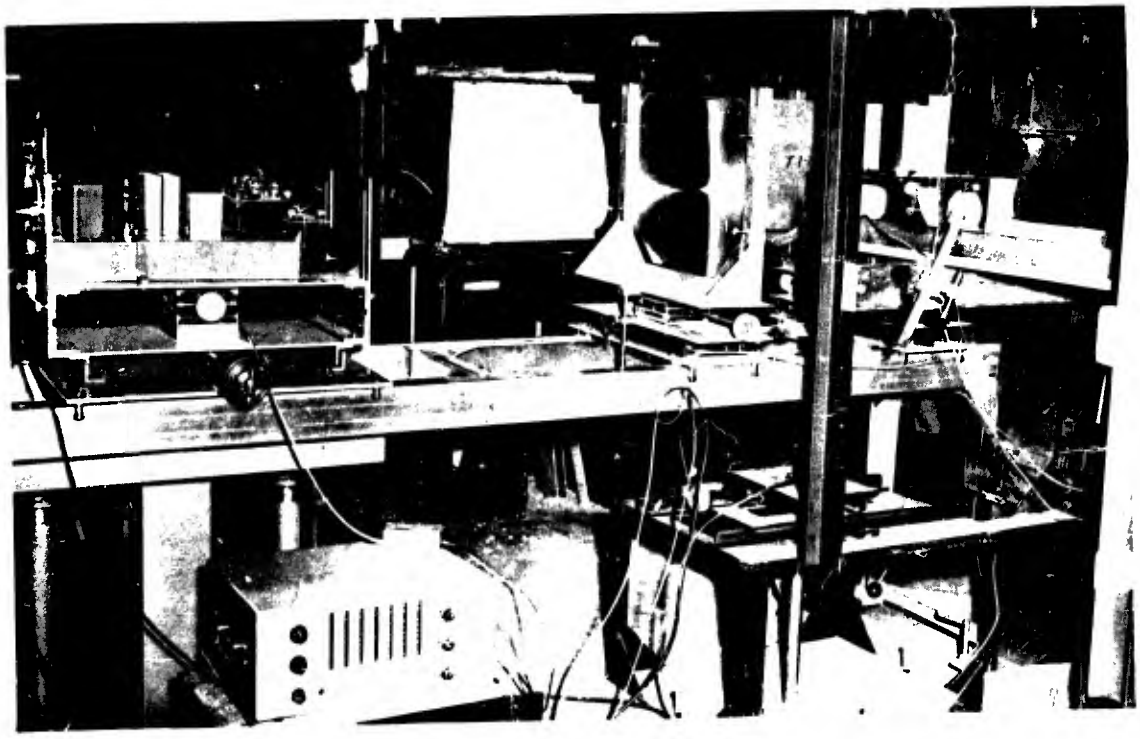

Figure 14. Photo-optical system set up in Ballistic Range (side view).

b. System calibration

The system is calibrated in order to determine the ratio of distance in the light field to distance on the photograph (i.e., the magnification for the system) and to check the spark time interval.

The magnification is determined by placing in the light field (parallel to the Fresnel lenses) a transparent plastic sheet on which has been ruled a grid of parallel, evenly spaced lines. The grid is then photographed and the magnification determined for seven positions within the field: three positions 1-inch apart on each side of the line of flight, and one on the line of flight itself. This spread is used since this is the maximum deviation of missile path as determined empirically. An average magnification is then determined.

The spark time interval is determined by attaching a counter to the spark unit, as shown in Figure 3. It was found necessary to attenuate the 200-volt pulse from the spark unit in order to use the 10-megacycle counter, although no attenuation is necessary for use with a 1.6-megacycle counter. Since we are measuring an interval, the length of leads from the counter to the spark unit should not affect our reading accuracy, provided the stop and start pulses are the same shape and the delay in each circuit is the same.

Another method for measuring the spark time interval is one in which the signal resulting from light pulses from the unit in Figure 15 goes directly to the start and stop terminals of a counter (Fig. 16). However, in this method the start signal from the first light pulse is delayed a fraction of a microsecond by a longer cable length, thus allowing the stop pulse to be dissipated before the start pulse starts the counter. Since the counter has already been started, the arrival of the signal from the second light pulse will stop the counter. The error in using this method is caused by the fractional microsecond delay and is negligible.

The measurement of distance on the photograph is made with dividers and a 60-lines-per-inch scale. Measurements are made to the nearest 120th of an inch and from the center of one projectile to the center of the other. We found that we could estimate the projectile center to the nearest 120th of an inch. The center-to-center measurements are made, rather than end to end, since projectiles are usually tipped. With the 17- by 22-inch Fresnel lenses (40-in focal length), 10-inch camera lens, and 3-1/4 by 4-1/4 inch film ordinarily used, a field size of 8 inches (in the direction of projectile movement) is photographed. In order to facilitate the "capture" of projectiles on the film, a 6-inch interval between successive sparks is sought. This corresponds to approximately 3 inches between projectile images on the film.

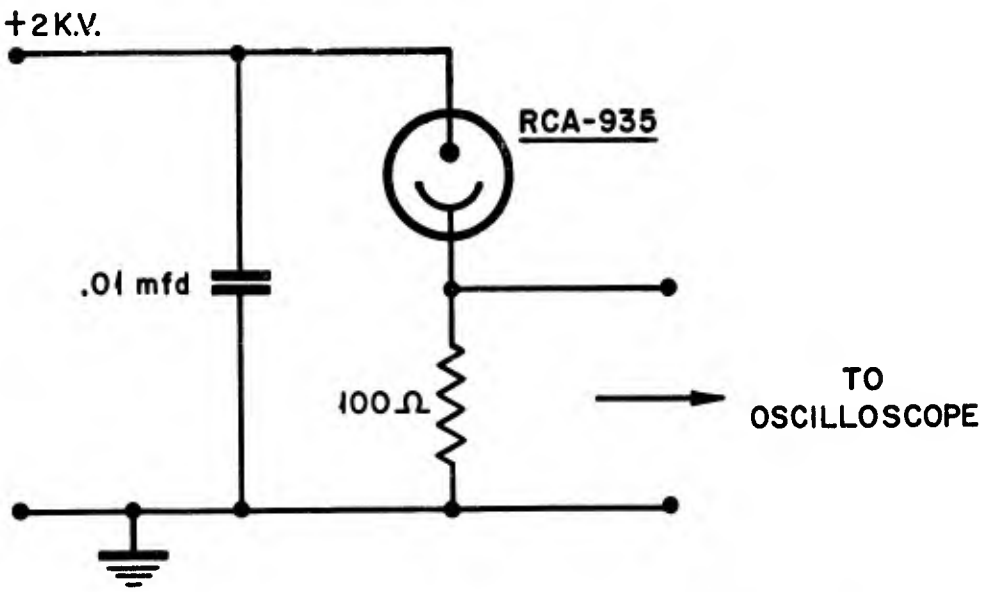

Figure 15. Schematic diagram of photoelectric calibrator.

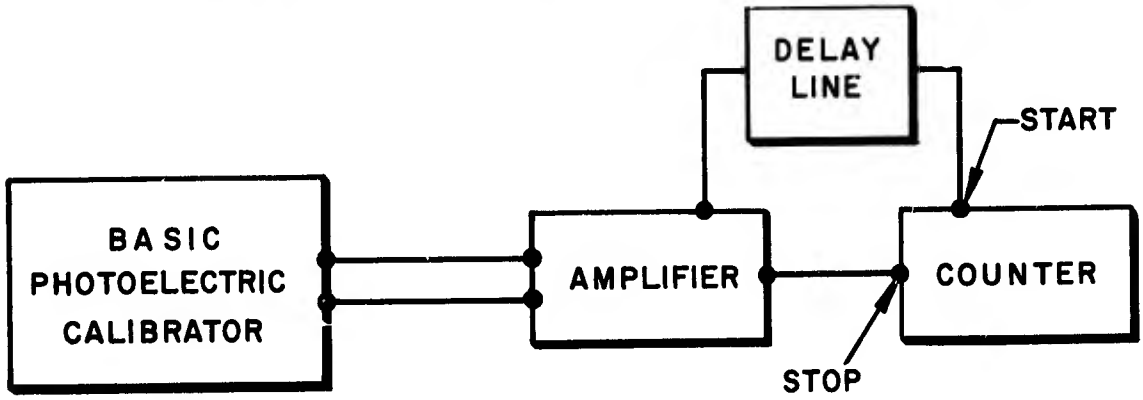

Figure 16. Schematic diagram of photoelectric unit for measuring spark interval.

C. Results

a. Image quality

An estimate of the angular deviation of the light in the field was determined from the image formation of the second Fresnel lens. The maximum angular deviation was calculated by using the deviated ray from the periphery of the lens. This deviation was approximately 28 minutes.

Since the camera focus is held constant, there is no noticeable variation in the magnification of the image resulting from spherical aberration causing non-parallel light within the field. There is, instead, a change in the focus of an image as the object within the field is deviated horizontally from the line of flight (for which the best camera focus has been obtained). This, coupled with increased curvature of the field, results in poorer image resolution for such deviated objects. Since the maximum deviation (for normal firings) of projectiles from the line of flight is 1 degree, the image resolution is only slightly impaired. The deviation, however, does change slightly the magnification resulting from distortion. This is illustrated in Figure 22 (p. 34).

The greatest sensitivity of the shadowgraphic system is achieved when the focal spot (the"focal spot", in this case, is actually an image of the spark) of the second Fresnel lens is centered at the surface of the camera lens. This is due to the large magnification at the focal point of any light deviations that are within the parallel-light field.

b. Resolution

The overall resolution, as illustrated in Figure 18a (photograph taken with 5-in focal length camera lens) is rather poor when compared to that of other photographic systems. However, the resolution is sufficient to enable the identification of various particles, projectile deformation, and the adequate location of measurement points (i.e., projectile centers).

Greater than 100 lines/inch can be resolved on the film, although with the combination of camera and film, an object of only 60 lines/inch can be resolved (Fig. 17a). With the complete photo-optical system, an object of only 30 lines/inch can be resolved consistently (Fig. 17b).

c. Impact light

Target impact flash and glowing particles have been attenuated to some extent. Figure 11, a photograph taken on standard panchromatic film with an open-shutter camera, shows target impact flash and glowing particles produced when a 17-grain fragment-simulator

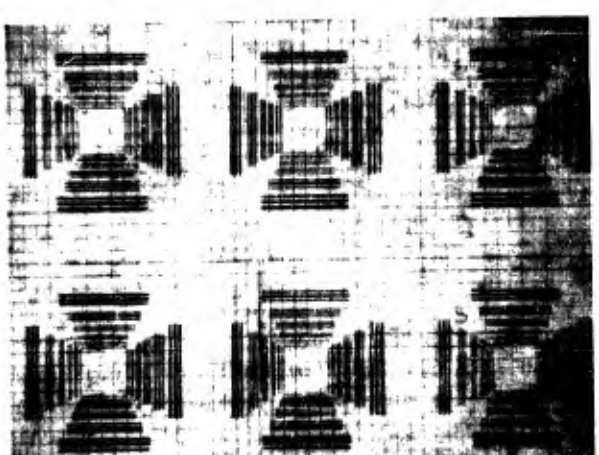

a. Chart taken with the camera alone.

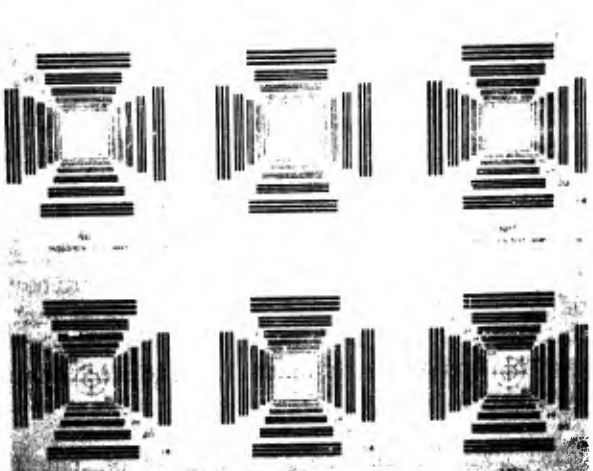

b. Chart in the field.

Figure 17. Resolution of image.

impacted a titanium alloy sheet. Figure 18 shows target impacts taken simultaneously: 1) through the photo-optical system (above), and 2) at 90 degrees to the optical system (below) with an open-shutter camera alone, using Polaroid film. Since, in most cases, there is little light flash on the exit side of the target, we may fire at targets directly within the light field and still obtain residual velocity data. This is a great advantage when it is necessary to determine the velocity of irregular punchout particles, since no drag correction is necessary.

In Figure 19, the difference in light attenuation resulting from the use of Kodak filter C-5 No. 47 is compared to that using Corning filter No. 5113.

d. Magnification

Figure 20 indicates the magnification variation for different positions* in the light field considering three different measuring distances (base lines on the film). Measurements were made for a constant lateral film position at the center of the lens. It will be noted that use of the largest base line (3 inches) results in the least variation of magnification.

Figure 21 indicates the magnification variation for different positions in the light field, using a 3-inch measuring distance at three different positions on the film. It is seen that the least variation in magnification occurs along the center line of the lens, although there is no extreme variation above or below the center line.

Figure 22 indicates the frequency of occurrence of a particular magnification in a series of twenty random measurements. It will be noted that the average of these is close to the magnification that occurs most frequently.

e. Spark-time interval

The spark-time interval, as determined by an electronic counter (connected directly to the double-spark unit), was compared with that of the actual light pulse interval (determined by a photocell and oscilloscope) over a range of 50 microseconds, since within this range the oscilloscope was accurate to 1 microsecond only. The difference in time interval measured by the two methods was 1 microsecond over the entire range.

* See second paragraph of system calibration (Section 4b)

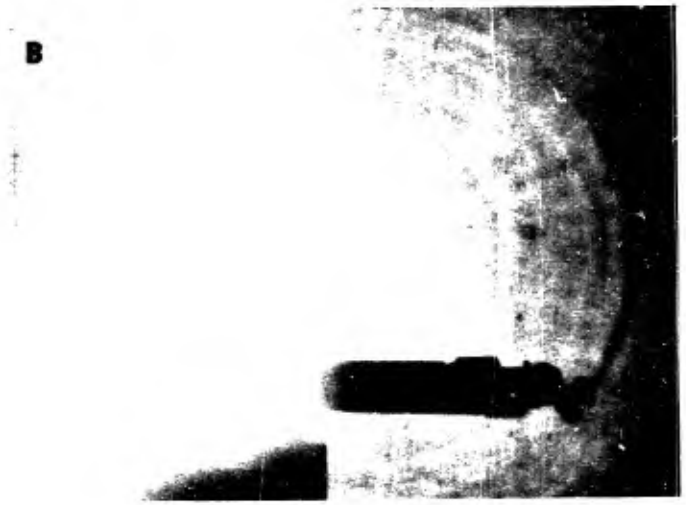

Figure 18. Two target impacts (A,C; B,D) as photographed through the optical system (A,B) and at right angles to the system (C,D)

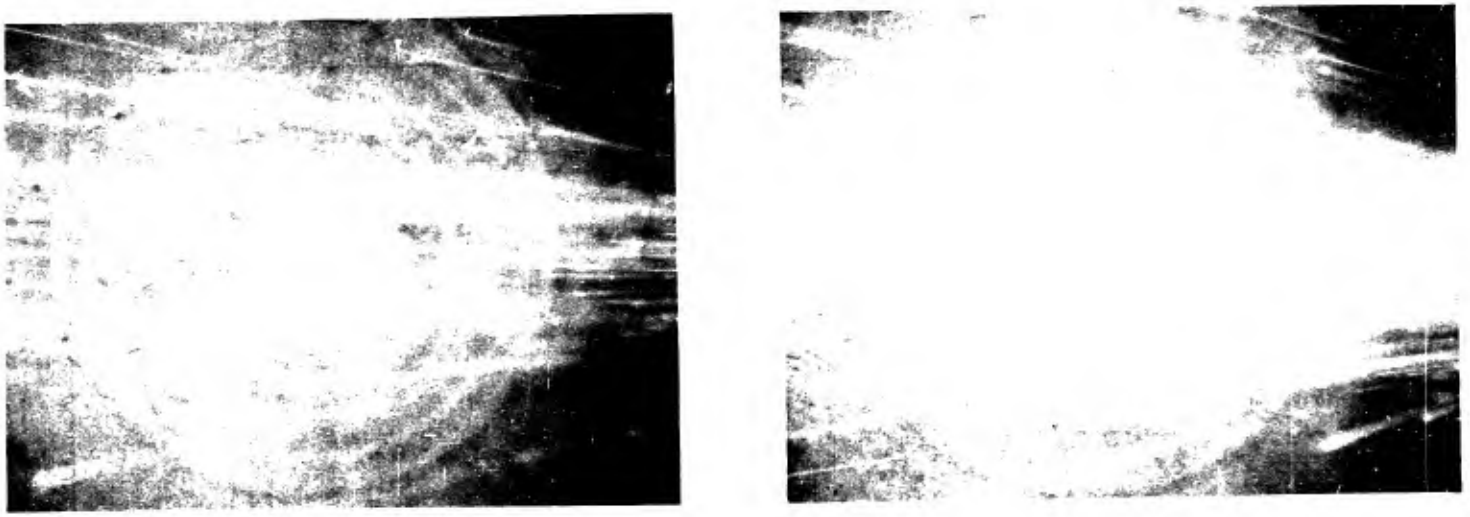

a. Corning 5113 filter

b. Kodak C-5 filter

Figure 19. Comparison of filters with titanium being impacted.

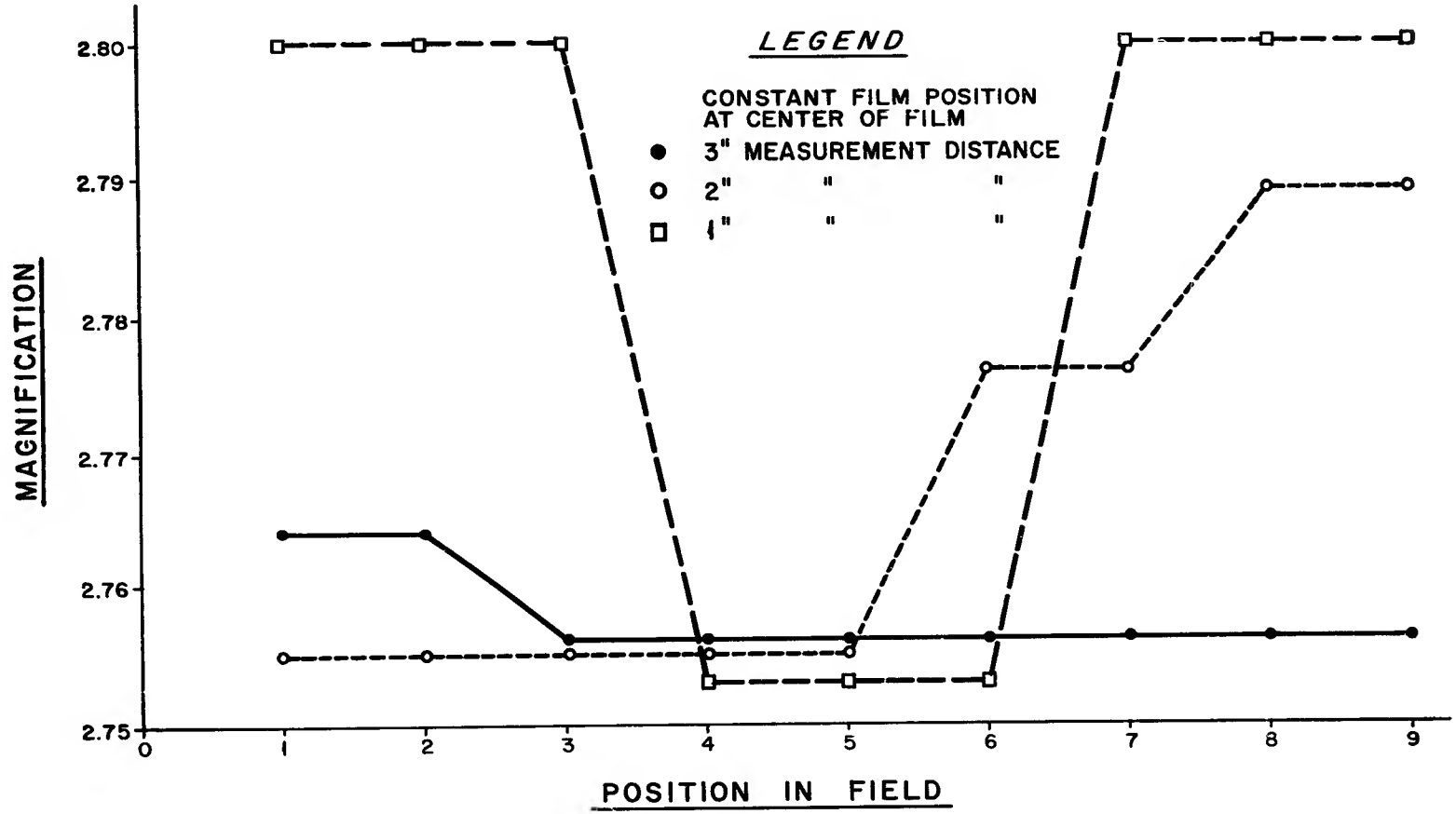

Figure 20. Magnification versus light field position for constant film position

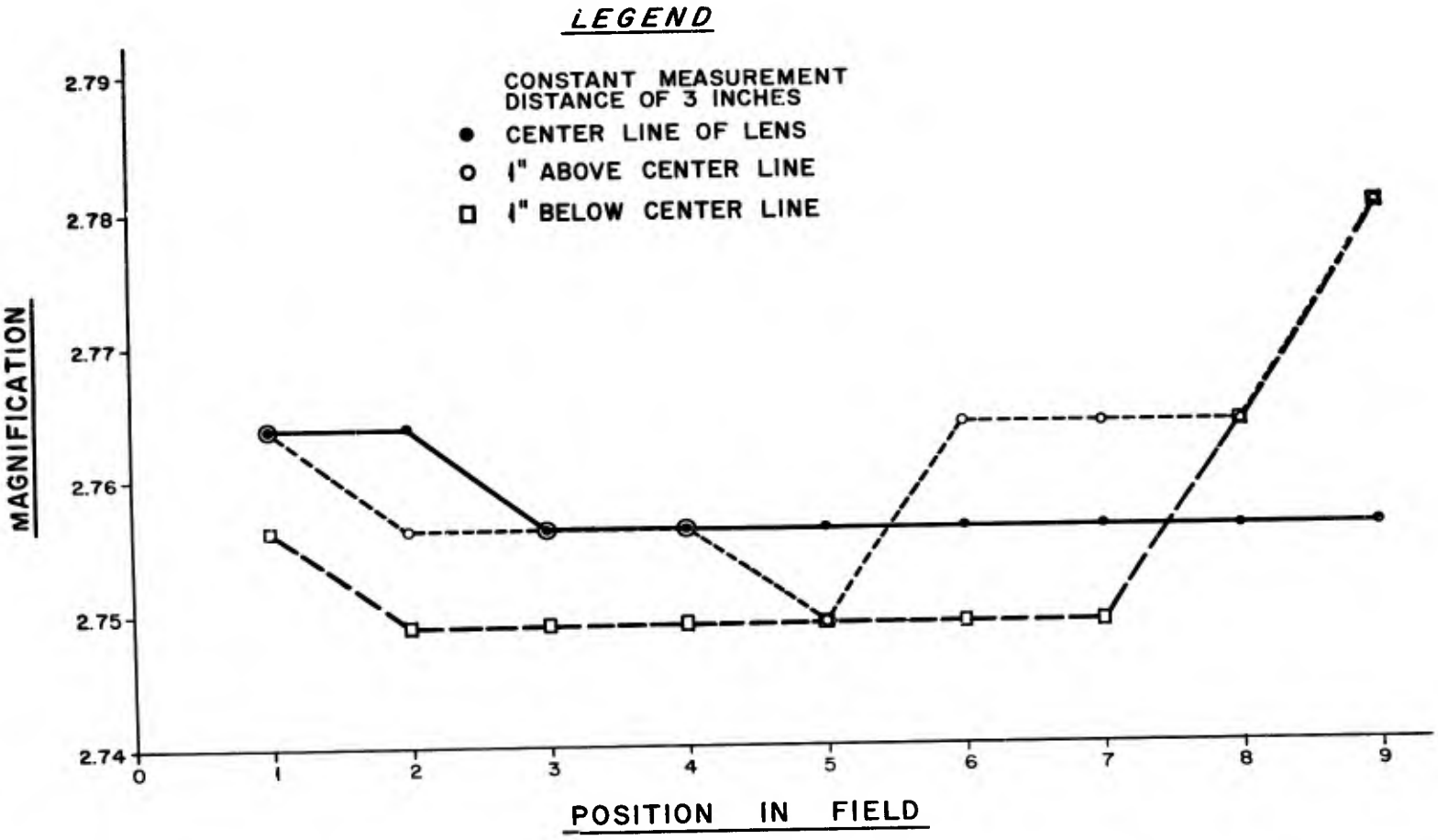

Figure 21. Magnification versus light field position for constant measurement distance.

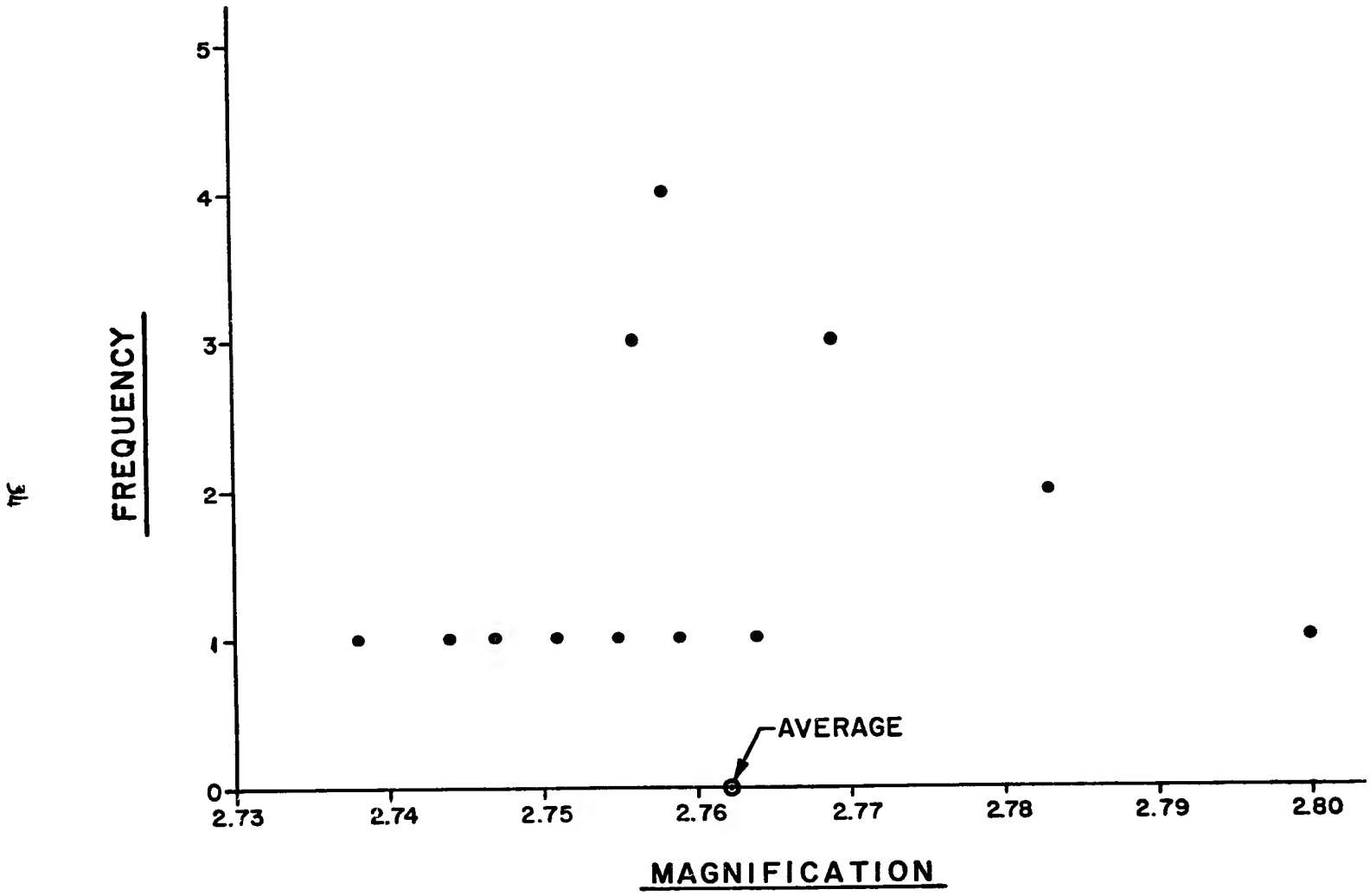

Figure 22. Frequency of occurrence of magnification for a series of random measurements.

f. Velocity comparison

The photo-optical system was compared with a silver-grid-paper projectile-velocity-measurement system, since the latter has a maximum error of only 0.5 percent.

Figure 23 shows velocity measured by the "grid" system plotted against the difference in velocities between the "grid" system and photo-optical system. Velocities were measured at the same point simultaneously by both systems for four velocity ranges. The maximum velocity differences are 1.4 percent at 3400 ft/sec, 1.3 percent at 3000 ft/sec, and 1.1 percent at both 2000 ft/sec and 1000 ft/sec. In many instances, however, the differences are less than 1 percent, as indicated by the points above the 1 percent difference line. It would appear that the error in spark-time interval was primarily responsible for the variation in velocity differences, since the time base decreases with velocity increase and the percentage difference varies in about the same way as the velocity difference.

For additional comparison, the "grid" system was compared to a light-screen projectile-velocity-measurement system. The differences, as shown in Figure 24, are less than 1 percent for all velocity ranges.

g. Calculated velocity and drag error

From Equation (9) of Appendix C we have:

$$\frac{\Delta v}{v} = \frac{(\Delta X_p + 2S)}{X_p} + \frac{(\mathrm{I} + \Delta \bar{X})}{M} + \frac{(\Delta C + \Delta u)}{t}$$

where

v = projectile velocity (ft/sec)

Δv = the uncertainty in velocity

ΔX_p = uncertainty in measurement of the photograph distance X_p (0.25 ft)
= 0.001 ft

S = additional uncertainty in measurement on the film due to spherical aberration blurring.
= $2S$ = 0.0016 ft.

I = uncertainty in magnification due to distortion (average deviation of randomly chosen magnification).
= 0.0024

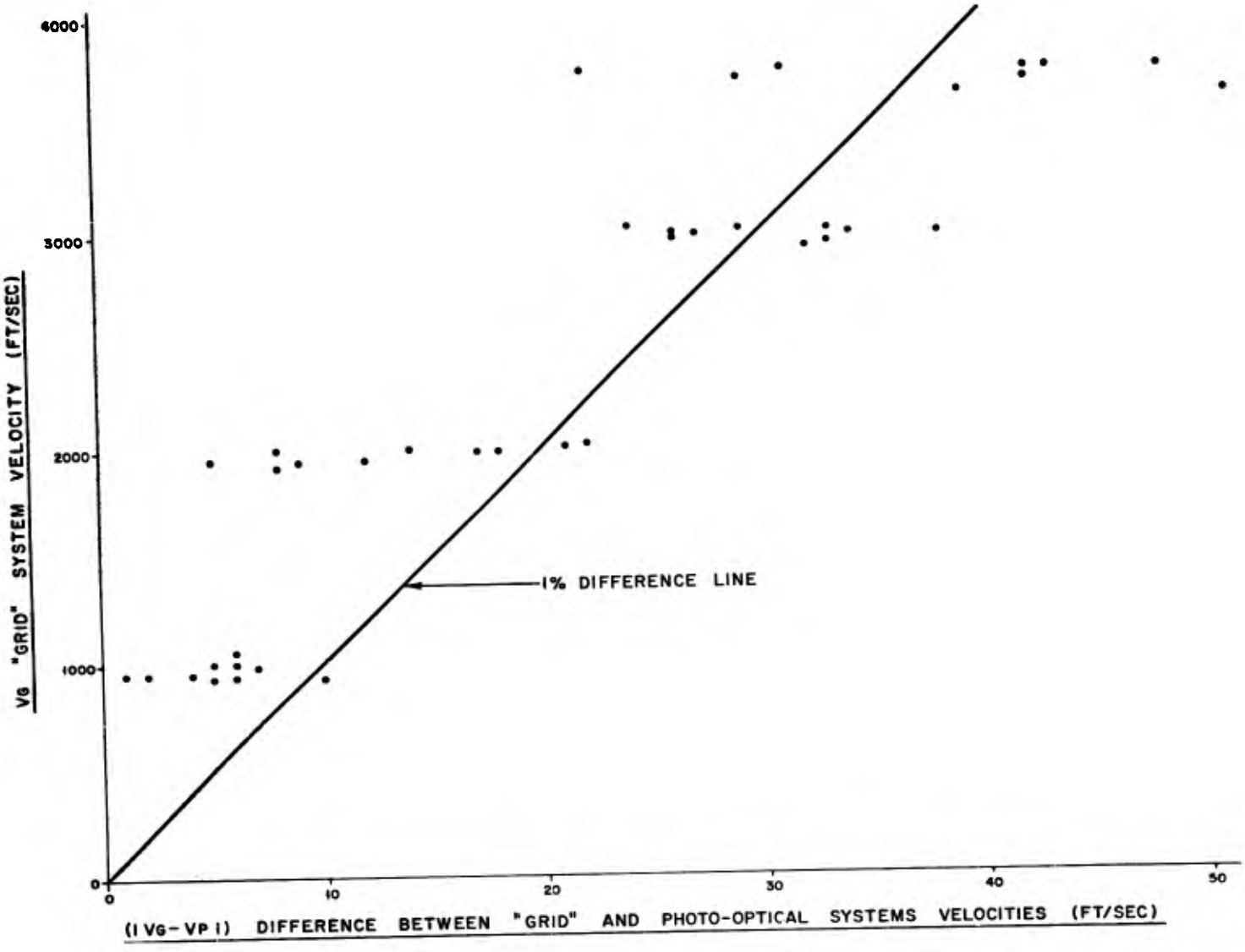

Figure 23. Difference in projectile velocity as measured by photo-optical and "grid" systems

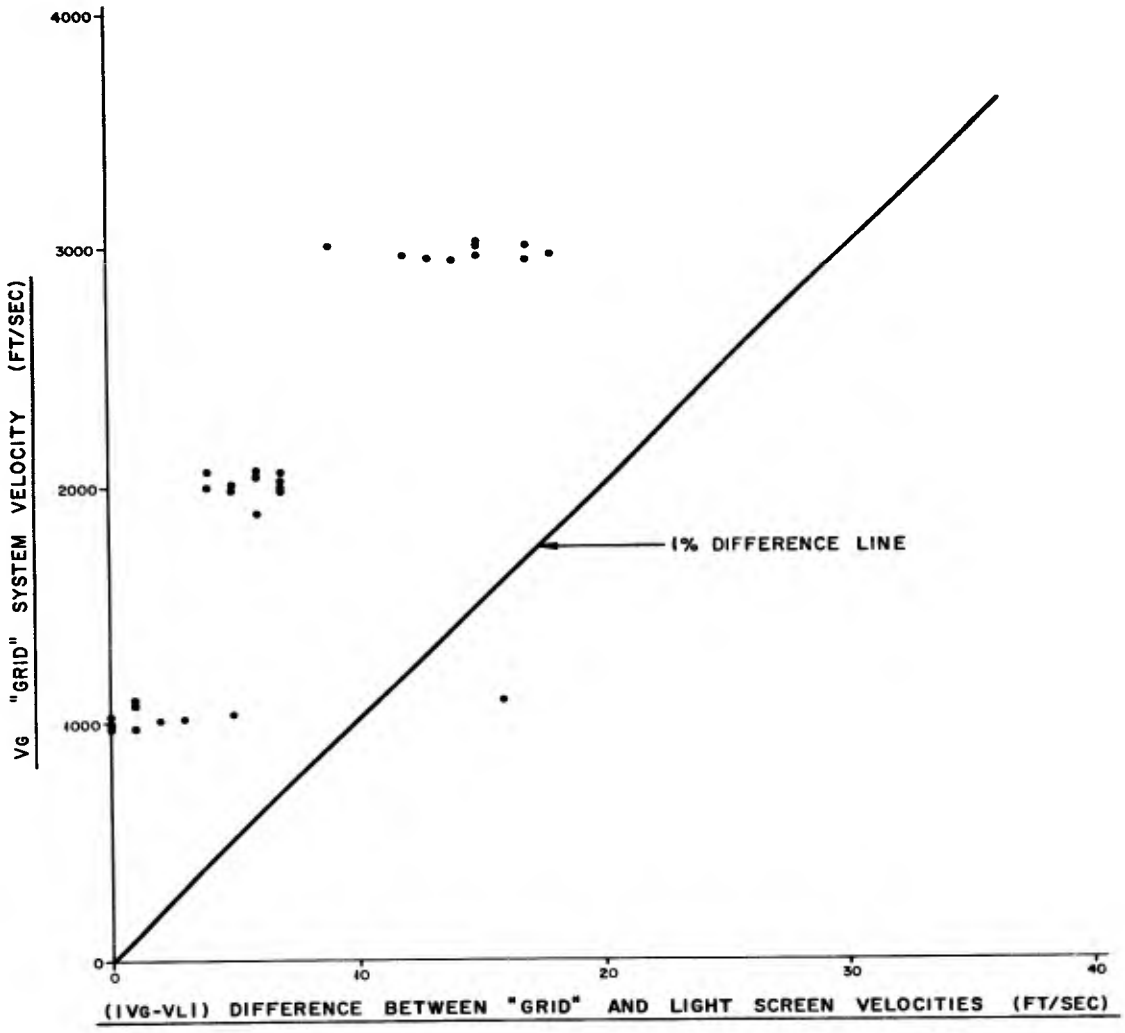

Figure 24. Difference in projectile velocity as measured by light screen and "grid" systems

ΔX = uncertainty in magnification due to error in measurement on the calibration grid
= 0.0033

M = magnification (image demagnification)
= 2.763

ΔC = an uncertainty in the time interval due to counter error
= 0.2×10^{-6} sec

Δu = an uncertainty in time interval due to an unsymetrical delay in start and stop circuit of the counter, spark unit, or connecting cables (can be made negligible)

t = spark-time interval 200×10^{-6} sec would result in a velocity within the 3000 ft/sec range

$$\frac{\Delta v}{v} = \frac{0.0026}{0.25} + \frac{0.0057}{2.763} + \frac{.2 \times 10^{-6}}{200 \times 10^{-6}}$$

$$\frac{\Delta v}{v} = 0.0135 = 1.35\%$$

This value, 1.35 percent, is comparable to the maximum error obtained from a comparison of the "grid" and photo-optical systems.

The fraction of (drag) error* in using

$$V = V_I \left(1 - \frac{S}{R}\right)$$

where: V_I = velocity measured at the transducer.

instead of: $V = V_I e^{-S/R}$

may be approximated by the third term in the $e^{-S/R}$ series.

$\therefore$ for $S = \frac{R}{16}$

$$E \approx \frac{1}{2}! \left(\frac{1}{16}\right)^2 = \frac{1}{512} = 0.00195$$

which is an error of approximately 0.2 percent.

*This was pointed out in a letter by Mr. John W. Jameson of the Body Armor Branch, Biophysics Division. U. S. Army Chemical Laboratories, Edgewood, Maryland.

The error attributable to moderate changes in the drag coefficient by using, for example, 0.0055 instead of 0.0062 for $\hat{R}$ in Equation (4), of Appendix A for a velocity of 3000 ft/sec (using a 17-grain fragment simulator) is less than 0.1 percent.

It has also been shown that for the 1- and 2-foot baselines that we use, the effect of drag displacing the actual measurement point from the center of the system (from which we measure for drag correction) is negligible.

The equation*, derived from Equation (2) Appendix A, is:

$$\rho = \eta \ln [\eta (e^{\frac{1}{\eta}} - 1)]$$

where:

ρ = the actual point at which the velocity measured by two transducers, separated by a distance (B), is located.

η = a constant indicating the number of times which the base line (B) must be increased to result in the distance for which the projectile velocity is diminished by e (2.718).

For the 1-foot baseline (B), $B \approx \frac{1}{90} \hat{R}$

therefore $\rho \approx 0.50007$ feet (compared to the normally employed value of $\frac{B}{2} = 0.50000$).

Since the errors in drag coefficient (18) (for the fragment simulator), density of air, and projectile angular deviation (at the "grid" system) are negligible, we may write Equation (10) of Appendix C quantitatively as a maximum of:

$$\Delta (V_S - V_R) = \Delta V_\rho + \Delta V_g + \Delta V_N$$

$$\Delta (V_S - V_R) = 1.35\% + 0.5\% + (0.4\% + 0.5\%)$$

$\Delta (V_S - V_R) = \underline{2.75\%}$. This is the maximum error in determining the striking and residual velocity difference, when using a grid system to determine V_S and the photo-optical system for V_R.

*Ibid

Figures 25 through 29, illustrating respectively: a) sensitivity for recording shock wave phenomena, b) the length of time which a projectile remains in contact with a target (impact time), and c) stress propagation under ballistic impact, indicate the versatility of the photo-optical system.

6. Summary

The advantages of the photo-optical system are as follows:

a. This method enables us to determine tumbling, change in path, and distortion of the projectile.

b. We can view the flight of other particles preceding or following the projectile and determine their velocities, size, shape, amount, and distribution

c. Residual velocity measurements can be made with an error of only approximately 1 to 2 percent.

d. The system is not elaborate and is relatively inexpensive.

e. Through the use of Polaroid film, data are immediately available.

f. At velocities above the speed of sound, shock wave measurements may be used to corroborate velocity measurements (see Appendix B).

g. Since our system uses a parallel light field, the size of an object will be viewed by the camera as the same no matter where it is within the field, providing that it is parallel to the Fresnel lenses. For approximately a 9-degree deflection (which is rather large), the error is 1 percent. In general, the deflections are a fraction of a degree. In many cases we may, therefore, neglect deflection of the projectile by the target and still achieve an accuracy in our velocity measurement that is reasonable for most purposes.

h. We may easily and inexpensively (to a large extent) attain wide fields of view merely by increasing the size of the Fresnel lenses and the focal length of the camera lens.

i. The system is readily adaptable to Schlieren techniques.

j. Any light produced within the lens field will be out of focus and therefore diminished.

k. Upward or downward deviations of the projectile cause no error in measurement.

l. There is good resolution of shock wave phenomena even from small particles, as illustrated in Figure 25c.

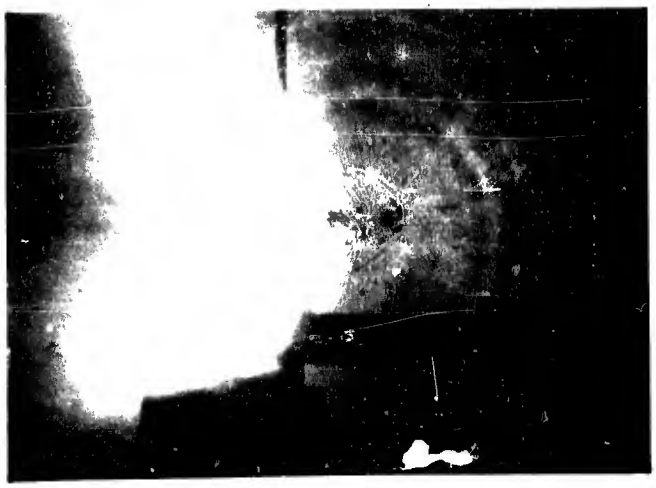

a

b

c

Figure 25. Sensitivity of the system for recording shock wave phenomena.

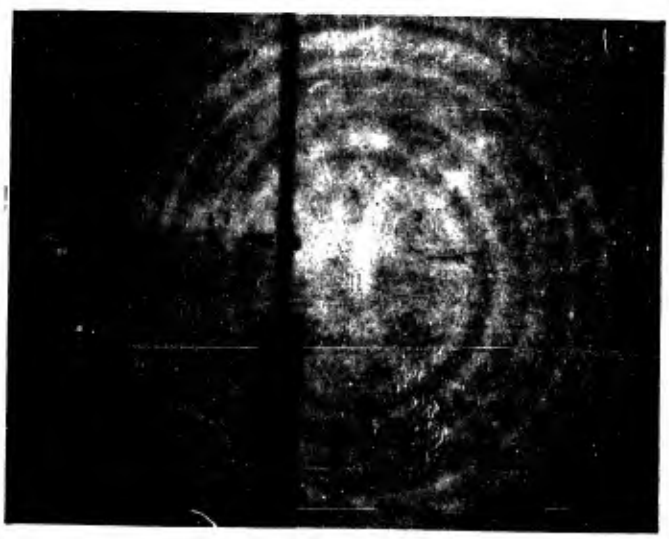

Figure 26. Impact of 1/8-inch aluminum by a 17-grain fragment simulator traveling at 1059 ft/sec. The time interval between missile images is 35 microseconds.

Figure 27. Stress propagation in CR-39 a short time after impact by a 17-grain fragment simulator at 1921 ft/sec. Taken with the photo-optical system using circularly polarized light. The arrow indicates the point of impact.

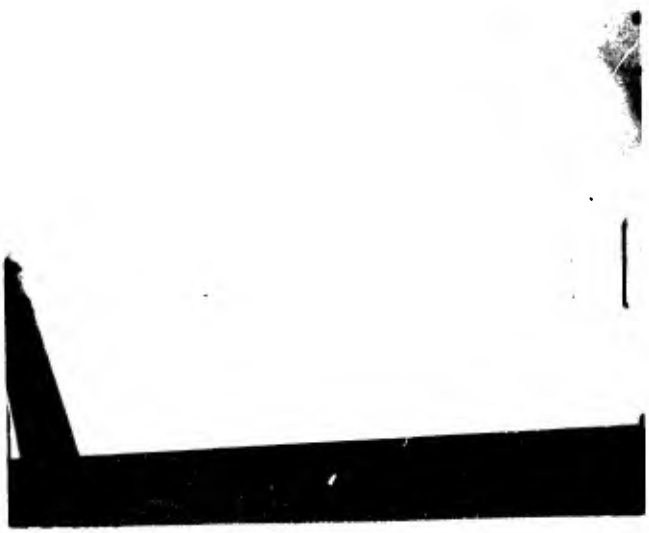

Figure 28. Reconstruction of impacted 1/4-inch CR-39 which was impacted on edge while clamped just below impact point.

Figure 29. Additional photograph of a 17-grain fragment simulator impacting CR-39 in the polarized light field, showing fringes.

7. References

1. Meyer, E. A. and N. J. Hanson. "Information Regarding the Energy Absorbing Characteristics of Materials for Utilization in Armor." Res Rpt First Quarter, Personnel Armor Branch, QM R&E Comm, Natick, Mass., 30 Jun 1957

2. Grossman, D. "Ballistic Velocity Instrumentation System Devised for Use at the Biophysics Div, Army Chemical Center." Rpt. 2081, Army Chemical Warfare Labs, Edgewood, Md. (1956)

3. Bailey, S. O., et al. "Facilities and Instrumentation of the NRL Hypervelocity Lab." Rpt. 5271, Naval Research Lab, Wash, D. C., 18 Feb 1959, p 6

4. Hall, D. A. "Photographic Method for Hypervelocity Measurements." Vol. I, Series II, "Instrumentation of High-Speed Photography." Soc. Motion Picture and Television Eng. (1960)

5. Wyckoff, C. "Exposure Reciprocity Effects on Several Photographic Films." Tech Memo B-289, Edgerton, Germeshausen & Grier, Inc., Boston, Mass., Sep 1960

6. Miller, O. E., et al. "Thin Sheet Plastic Fresnel Lenses of High Aperture." J. Optical Soc. of Amer, 41 (11) 807-815, Nov 1951

7. Edgerton, H. E. and F. E. Barstow. "Multiflash Photography." Photographic Science and Engineering, 3 (6) Nov-Dec 1959

8. Beckman & Whitley Tech Data Sheet, Beckman & Whitley, Inc., San Carlos, California, 1961

9. Edgerton, H. E., et al. "Submicrosecond Flash Sources." Fifth Int'n'l Congress on High-Speed Photography, Wash, D. C., 16-22 Oct 1960

10. Partridge, W. S. "Construction of a High Velocity Gun for Propelling Small Irregular-Shaped Pellets." Interim Tech. Rpt. 8, Dept of Electrical Engineering, Univ of Utah, Salt Lake City, Utah, Mar 1957

11. Früngel, Frank. "High-Speed, Slow-Motion Pictures by Means of Spark Flashes." Explosivstoffe No. 10 (1958)

12. Edgerton, H. E. and C. Wyckoff. "A Rapid Action Shutter with No Moving Parts." Journal Soc. Motion Picture and Television Eng, 56, April 1951

13. Courtney-Pratt, J. S. "A Review of the Methods of High-Speed Photography." Rpt. on Progress in Physics, 20, The Physical Society, Great Britain (1957)

14. Wilson, M. R. and R. J. Hiemenz. "Light Source for High-Speed Photography." Research Trends, 3, Cornell Aeronautical Lab, Inc., Buffalo, N. Y. (1959)

15. Librascope Tech Data Sheet. Librascope, Inc., Livermore, Calif (1960)

16. Avco Tech Data Sheet. Avco Res.& Advanced Dev. Div., Wilmington, Mass (1960)

17. Winch, R. P. "Electricity & Magnetism." Prentiss-Hall Publishers, New Jersey (1958)

18. Tente, A. S. "Experimental Determination of the Drag Factor for the T-37, .22-Cal Frag Simulator." Textile Eng.Rpt.182, QM R&D Comm, Natick, Mass. (1957)

19. Dodge, R. A. and M. J. Thompson. "Fluid Mechanics." McGraw Hill Book Co., Inc., N. Y. C. (1937)

20. Chesterman, W. D. "The Photographic Study of Rapid Events." Clarendon Press, Oxford, England (1951)

21. General Radio Catalogue, General Radio Co., W. Concord, Mass. (1961)

8. Acknowledgments

The author wishes to express his appreciation to the many individuals of the Instrument Shop, Machine Shop, and Ballistics Range for their support in the construction and testing of the photo-optical system, and to Mr. Anthony Alesi, of the Materials Research Branch, for his review of the manuscript.

APPENDIX A

PROJECTILE VELOCITY CORRECTION DUE TO AIR DRAG

F = drag force

K_D = drag coefficient

m = mass of projectile

v = instantaneous velocity

ρ = relative air density

a = acceleration

A = projected area of missile

$$D = F = ma = W\frac{dv}{dt} = K_D \rho A v^2 \qquad (1)^*$$

$$\frac{dv}{dt} = \frac{K_D \rho v^2}{w} \qquad \text{where: } v = \frac{ds}{dt}$$

let:
$$\frac{K_D \rho A}{w} = \frac{1}{R}$$

$$\frac{dv}{dt} = \frac{1}{R} v^2 = \frac{1}{R} v \cdot v$$

$$\frac{dv}{dt}\frac{1}{v} = \frac{1}{R}\frac{ds}{dt}$$

when: $t = t_s$, $v = V_s$ and $s = S$

where: t_s is the time taken to travel some distance (S) downrange.

therefore:

$$\int_{v=V}^{v=V_s} \frac{dv}{dt}\frac{1}{v}\,dt = \frac{1}{R}\int_{s=0}^{s=S} ds$$

$$\ln V = -\frac{S}{R} + \ln V_s$$

$$\boxed{V = V_s\, \varepsilon^{-S/R}} \qquad (2)$$

$$\varepsilon^{-S/R} = 1 - \left(\frac{S}{R}\right)\frac{1}{1!} + \left(\frac{S}{R}\right)^2 \frac{1}{2!} - \cdots\cdots$$

*For derivation of Equation (1), see reference 19.

Taking only the 1st two terms as an approximation, and substituting in (2), we have:

$$V = V_s \left(1 - \frac{S}{R}\right)$$

$$V = V_s \left(1 - \frac{S K_D \rho A}{W}\right) \qquad (3)$$

for a particular missile: $\frac{W}{A}$ = a constant

letting: $k = \frac{K_D A}{W}$ we may write for a particular missile:

$$V = V_s \left(1 - S k \rho\right) \qquad (4)$$

If we take ρ (the relative air density) = 1 and k* (for 22 cal. frag. sim.) = .0055

we have: $$V = V_s \left[1 - S(0.0055)\right]$$

It should be noted that the K_D which we use is an average figure for a particular range of velocities and at a particular temperature and relative humidity. The K_D varies somewhat even within the chosen velocity range, although this introduces little error for a projectile with the geometry and weight of the fragment simulator. For smaller and lighter projectiles, however, any variation in air drag becomes much more significant. Therefore, atmospheric conditions should be held relatively constant and the K_D for the particular projectile velocity should be used in computing the air drag for small projectiles.

*See Ref. 18

APPENDIX B

SHOCK WAVE VELOCITY MEASUREMENT

1) Draw tangents to shock wave as far back from the vertex as possible (linear portion of the shock wave).

2) Measure the angle (θ) from line of flight to shock wave tangent.

3) The velocity of the missile (V) is then given by:

$$V = \frac{\text{velocity of sound}}{\sin \theta} \quad (19)$$

This method is useful in approximating the velocity for a check on transducer systems. The velocity arrived at in this way may vary 200 or 300 ft/sec from the correct value.

APPENDIX C

ACCURACY OF THE VELOCITY MEASUREMENT

The error involved in velocity measurement is a function of the uncertainty in time and space measurements. In our system, we are concerned with the measurement of an average projectile velocity (v) given simply by:

$$v = \frac{x}{t} \tag{1}$$

where: x is the distance the projectile travels in a time, t. The uncertainty* given in (1) is then expressed as:

$$dv = \frac{dx}{t} - \frac{x\,dt}{t^2} \tag{2}$$

or in terms of relative error by:

$$\frac{dv}{v} = \frac{dx}{x} - \frac{dt}{t} \tag{3}$$

If the errors are very small compared to the total measurement, then we may replace the differentials by the small differences $\Delta v, \Delta x,$ and Δt.

Also, since the errors are random and since we are interested in the maximum error, we may write (2) as:

$$\Delta v = \frac{\Delta x}{t} + \frac{x}{t^2}\,\Delta t \tag{4}$$

Spacial Error

A distance in the paralled light field x is related to the image of this distance on the film x_p by:

$$x = M x_p \tag{5}$$

*It should be mentioned that we are primarily interested in the accuracy of each velocity measurement and not in the accuracy (consistency) in making a velocity measurement for a series of many measurements which might be expressed by the standard deviation of such a series of measurements. This is aside from the fact that we cannot obtain, with a high degree of accuracy, a particular projectile velocity (due to inconsistencies in powder, loading of cartridges, and varying projectile sizes).

where: M is the overall magnification of the system.

Using the same assumptions as in (4), the error in X is given by:

$$\Delta X = M\Delta X_p + X_p \Delta M \qquad (6)$$

The error involved in X_p is determined by the independent errors due to image blur, B, image resolution of system, R, the accuracy to which the measurement on the film is taken, ΔX_p, and an uncertainty of image size due to focal differences resulting from spherical aberration, S.

where: $B = \frac{v t_e}{M}$ $\quad v$ = projectile velocity

t_e = exposure time

In general, since two images are involved in the measurement of X_p,

$$\Delta X_p = 2B + \frac{2}{R} + \Delta X_p + 2S$$

Since the camera lens is in a fixed position, the spherical aberration will produce a slight image blurring rather than a change in image magnification, due to different projectile positions within the light field. The amount of blur in each image may be different; this is due to angular deviation within the light field resulting in the possibility of twice the error in estimating projectile centers.

Since image blur, B, (due to position change during spark interval) is essentially the same for each image, the uncertainty in determining the distance between images will be essentially the same as that for a non-blurred image. This will also be the case for image resolution. We may therefore write:

$$\Delta X_p = \Delta X_p + 2S$$

The errors involved in ΔM are due to a distortional error, D, and an error due to inaccuracy in the measurement on the calibration grid, ΔX, used to determine magnification (with reference to X_p). We may finally write ΔX as:

$$\Delta X = M\ (\Delta X_p)\ + X_p (D + \Delta X) \qquad (7)$$

Time Error

The factors involved in time error are: a) the counter error (ΔC) (which includes oscillator stability and circuit jitter); and b) any error due to unsymmetrical delay (ΔU) in the start and stop circuits or associated transmission lines.

Therefore: $\Delta t = \Delta C + \Delta U \qquad (8)$

Total Error in Velocity Measurement

Substituting (7) and (8) in (4) we have:

$$\Delta V = \frac{M(\Delta X\rho + 2S) + X\rho(\Pi + \Delta X)}{t} + \frac{X(\Delta C + \Delta U)}{t^2}$$

or since:

$$V = \frac{MX\rho}{t} = \frac{X}{t}$$

$$\frac{\Delta V}{V} = \frac{(\Delta X\rho + 2S)}{X\rho} + \frac{(\Pi + \Delta X)}{M} + \frac{(\Delta C + \Delta U)}{t} \qquad (9)$$

By decreasing the magnification, we may increase the actual base line, X , but we also decrease the accuracy of measuring X . It is therefore desirable to increase the film base line (allowing greater magnification while still maintaining a large X).

In order to obtain the entire error in our measurement of velocity, we must add the non-system variables:

Δk = error in drag coefficient

d = error in drag equation

a = error due to angular deviation

$\Delta\rho$ = error in air density variation

where:

$$\Delta V_N = (\Delta k + d + a + \Delta\rho)$$

The error, therefore, in determining ($V_S - V_R$), using the grid system for V_S and the photo-optical system for V_R , could be a maximum of:

$$\Delta(V_S - V_R) = \Delta V_\rho + \Delta V_g + \Delta V(N_\rho) + \Delta V(N_g) \qquad (10)$$

where:

$\Delta V(N_\rho)$ = error due to non-system variables at photo system

$\Delta V(N_g)$ = error due to non-system variables at grid system

ΔV_S = striking velocity error

ΔV_R = residual velocity error

ΔV_ρ = photo-optical system velocity error

ΔV_g = "grid" system velocity error

UNCLASSIFIED